32. Rohr, O., C. Marban, D. Aunis, and E. Schaeffer. 2003. Regulation of HIV-1 gene transcription: from lymphocytes to microglial cells. *J. Leukocyte Biol.* 74: 736–749.
33. Okamoto, T., T. Matsuyama, S. Mori, Y. Hamamoto, N. Kobayashi, N. Yamamoto, S. F. Josephs, F. Wong-Staal, and K. Shimotohno. 1989. Augmentation of human immunodeficiency virus type 1 gene expression by tumor necrosis factor α. *AIDS Res. Hum Retroviruses* 5: 131–138.
34. Takada, N., T. Sanda, H. Okamoto, J. P. Yang, K. Asamitsu, L. Sarol, G. Kimura, H. Uranishi, T. Tetsuka, and T. Okamoto. 2002. RelA-associated inhibitor blocks transcription of human immunodeficiency virus type 1 by inhibiting NF-κB and Sp1 actions. *J. Virol.* 76: 8019–8030.
35. Urzainqui, A., J. M. Serrador, F. Viedma, M. Yanez-Mo, A. Rodriguez, A. L. Corbi, J. L. Alonso-Lebrero, A. Luque, M. Deckert, J. Vazquez, and F. Sanchez-Madrid. 2002. ITAM-based interaction of ERM proteins with Syk mediates signaling by the leukocyte adhesion receptor PSGL-1. *Immunity* 17: 401–412.
36. Fodor, S., Z. Jakus, and A. Mocsai. 2006. ITAM-based signaling beyond the adaptive immune response. *Immunol. Lett.* 104: 29–37.
37. Underhill, D. M., and H. S. Goodridge. 2007. The many faces of ITAMs. *Trends Immunol.* 28: 66–73.
38. Dimitrov, D. S., R. L. Willey, H. Sato, L. J. Chang, R. Blumenthal, and M. A. Martin. 1993. Quantitation of human immunodeficiency virus type 1 infection kinetics. *J. Virol.* 67: 2182–2190.
39. Chancey, C. J., K. V. Khanna, J. F. Seegers, G. W. Zhang, J. Hildreth, A. Langan, and R. B. Markham. 2006. Lactobacilli-expressed single-chain variable fragment (scFv) specific for intercellular adhesion molecule 1 (ICAM-1) blocks cell-associated HIV-1 transmission across a cervical epithelial monolayer. *J. Immunol.* 176: 5627–5636.
40. Farina, C., D. Theil, B. Semlinger, R. Hohlfeld, and E. Meinl. 2004. Distinct responses of monocytes to Toll-like receptor ligands and inflammatory cytokines. *Int. Immunol.* 16: 799–809.
41. Eitner, F., Y. Cui, G. Grouard-Vogel, K. L. Hudkins, A. Schmidt, T. Birkebak, M. B. Agy, S. L. Hu, W. R. Morton, D. M. Anderson, et al. 2000. Rapid shift from virally infected cells to germinal center-retained virus after HIV-2 infection of macaques. *Am. J. Pathol.* 156: 1197–1207.
42. Gray, C. M., J. Lawrence, E. A. Ranheim, M. Vierra, M. Zupancic, M. Winters, J. Altman, J. Montoya, A. Zolopa, J. Schapiro, et al. 2000. Highly active antiretroviral therapy results in HIV type 1 suppression in lymph nodes, increased pools of naive T cells, decreased pools of activated T cells, and diminished frequencies of peripheral activated HIV type 1-specific $CD8^+$ T cells. *AIDS Res. Hum Retroviruses* 16: 1357–1369.
43. Lu, W., X. Wu, Y. Lu, W. Guo, and J. M. Andrieu. 2003. Therapeutic dendritic-cell vaccine for simian AIDS. *Nat. Med.* 9: 27–32.
44. Schmitz, J., J. van Lunzen, K. Tenner-Racz, G. Grossschupff, P. Racz, H. Schmitz, M. Dietrich, and F. T. Hufert. 1994. Follicular dendritic cells retain HIV-1 particles on their plasma membrane, but are not productively infected in asymptomatic patients with follicular hyperplasia. *J. Immunol.* 153: 1352–1359.
45. Zhang, Z. Q., T. Schuler, W. Cavert, D. W. Notermans, K. Gebhard, K. Henry, D. V. Havlir, H. F. Gunthard, J. K. Wong, S. Little, et al. 1999. Reversibility of the pathological changes in the follicular dendritic cell network with treatment of HIV-1 infection. *Proc. Natl. Acad. Sci. USA* 96: 5169–5172.
46. Baroni, C. D., and S. Uccini. 1990. Lymph nodes in HIV-positive drug abusers with persistent generalized lymphadenopathy: histology, immunohistochemistry, and pathogenetic correlations. *Prog. AIDS Pathol.* 2: 33–50.
47. Houn, H. Y., A. A. Pappas, and E. M. Walker, Jr. 1990. Lymph node pathology of acquired immunodeficiency syndrome (AIDS). *Ann. Clin. Lab. Sci.* 20: 337–342.
48. Tsukamoto, K., Y. C. Huang, W. C. Dorsey, B. Carns, and V. Sharma. 2006. Juxtacrine function of interleukin-15/interleukin-15 receptor system in tumour derived human B-cell lines. *Clin. Exp. Immunol.* 146: 559–566.
49. Pilotti, E., L. Elviri, E. Vicenzi, U. Bertazzoni, M. C. Re, S. Allibardi, G. Poli, and C. Casoli. 2007. Postgenomic up-regulation of CCL3L1 expression in HTLV-2-infected persons curtails HIV-1 replication. *Blood* 109: 1850–1856.
50. Hidari, K. I., A. S. Weyrich, G. A. Zimmerman, and R. P. McEver. 1997. Engagement of P-selectin glycoprotein ligand-1 enhances tyrosine phosphorylation and activates mitogen-activated protein kinases in human neutrophils. *J. Biol. Chem.* 272: 28750–28756.
51. Weyrich, A. S., T. M. McIntyre, R. P. McEver, S. M. Prescott, and G. A. Zimmerman. 1995. Monocyte tethering by P-selectin regulates monocyte chemotactic protein-1 and tumor necrosis factor-α secretion: signal integration and NF-κB translocation. *J. Clin. Invest.* 95: 2297–2303.
52. Damle, N. K., K. Klussman, M. T. Dietsch, N. Mohagheghpour, and A. Aruffo. 1992. GMP-140 (P-selectin/CD62) binds to chronically stimulated but not resting $CD4^+$ T lymphocytes and regulates their production of proinflammatory cytokines. *Eur. J. Immunol.* 22: 1789–1793.
53. Tada, J., M. Omine, T. Suda, and N. Yamaguchi. 1999. A common signaling pathway via Syk and Lyn tyrosine kinases generated from capping of the sialomucins CD34 and CD43 in immature hematopoietic cells. *Blood* 93: 3723–3735.
54. Gilbert, C., C. Barat, R. Cantin, and M. J. Tremblay. 2007. Involvement of Src and Syk tyrosine kinases in HIV-1 transfer from dendritic cells to $CD4^+$ T lymphocytes. *J. Immunol.* 178: 2862–2871.

Virology 394 (2009) 64–72

Contents lists available at ScienceDirect

Virology

journal homepage: www.elsevier.com/locate/yviro

Selective infection of CD4$^+$ effector memory T lymphocytes leads to preferential depletion of memory T lymphocytes in R5 HIV-1-infected humanized NOD/SCID/IL-2Rγ^{null} mice

Chuanyi Nie [a,1], Kei Sato [a,1], Naoko Misawa [a], Hiroko Kitayama [a], Hisanori Fujino [b], Hidefumi Hiramatsu [b], Toshio Heike [b], Tatsutoshi Nakahata [b], Yuetsu Tanaka [c], Mamoru Ito [d], Yoshio Koyanagi [a,*]

[a] Laboratory of Viral Pathogenesis, Institute for Virus Research, Kyoto University, 53 Shogoinkawara-cho, Sakyo-ku, Kyoto, Kyoto 606-8507, Japan
[b] Department of Pediatrics, Graduate School of Medicine, Kyoto University, Kyoto, Kyoto 606-8501, Japan
[c] Department of Immunology, Graduate School of Medicine, University of the Ryukyus, Nishihara, Okinawa 903-0125, Japan
[d] Central Institute for Experimental Animals, Kawasaki, Kanagawa 216-0001, Japan

ARTICLE INFO

Article history:
Received 8 April 2009
Returned to author for revision 19 July 2009
Accepted 4 August 2009
Available online 9 September 2009

Keywords:
HIV-1 pathogenesis
Humanized mouse
Memory cell depletion
Productive infection
T cell activation

ABSTRACT

To investigate the events leading to the depletion of CD4$^+$ T lymphocytes during long-term infection of human immunodeficiency virus type 1 (HIV-1), we infected human CD34$^+$ cells-transplanted NOD/SCID/IL-2Rγ^{null} mice with CXCR4-tropic and CCR5-tropic HIV-1. CXCR4-tropic HIV-1-infected mice were quickly depleted of CD4$^+$ thymocytes and both CD45RA$^+$ naïve and CD45RA$^-$ memory CD4$^+$ T lymphocytes, while CCR5-tropic HIV-1-infected mice were preferentially depleted of CD45RA$^-$ memory CD4$^+$ T lymphocytes. Staining of HIV-1 p24 antigen revealed that CCR5-tropic HIV-1 preferentially infected effector memory T lymphocytes (T_{EM}) rather than central memory T lymphocytes. In addition, the majority of p24$^+$ cells in CCR5-tropic HIV-1-infected mice were activated and in cycling phase. Taken together, our findings indicate that productive infection mainly takes place in the activated T_{EM} in cycling phase and further suggest that the predominant infection in T_{EM} would lead to the depletion of memory CD4$^+$ T lymphocytes in CCR5-tropic HIV-1-infected mice.

Introduction

While it is evident that human immunodeficiency virus type 1 (HIV-1) causes acquired immunodeficiency syndrome (AIDS) in humans, the mechanism by which HIV-1 accomplishes this remains unclear. The gradual loss of peripheral blood (PB) CD4$^+$ T lymphocytes during the asymptomatic phase of HIV-1 infection is one of the best prognostic predictors for the onset of AIDS (O'Brien et al., 1996), and CD4$^+$ T lymphocyte depletion is thought to be a serious pathological change in AIDS (McCune, 2001).

To define the mechanisms behind CD4$^+$ T lymphocyte depletion, a large number of studies have been conducted in humans, primates, and humanized mice by using HIV-1, simian immunodeficiency virus (SIV), and SIV/HIV-1 chimeric virus (SHIV) (Centlivre et al., 2007; Koyanagi et al., 2008; McCune, 2001). One of the important findings from previous studies was the dependence of pathogenesis on the co-receptor preference, CXCR4, and/or CCR5 (Berkowitz et al., 1998; Moore et al., 2004). CXCR4-tropic (X4) SHIV caused rapid and complete depletion of all subsets of CD4$^+$ T lymphocytes in rhesus macaques, which led to death from immunodeficiency (Nishimura et al., 2004). On the other hand, CCR5-tropic (R5) HIV-1 is the dominant type of HIV-1 found in patients, and clinical manifestation of HIV-1 infection resembles CCR5-tropic SIV infection (Berger, Murphy, and Farber, 1999). In both HIV-1-infected patients and SIV-infected rhesus macaques, the drastic onset of immunodeficiency is rare (Ambrose et al., 2007; McCune, 2001), and CD4$^+$ T lymphocytes in PB slowly decrease in number, eventually leading to immunodeficiency.

X4 virus uses CXCR4 as the co-receptor and R5 virus uses CCR5 as the co-receptor for viral infection into target cells (Berger, Murphy, and Farber, 1999; Lusso, 2006). CXCR4 is expressed on naïve T lymphocytes and thymocytes, thus X4 HIV-1 can infect naïve T lymphocytes and thymocytes (Pedroza-Martins et al., 1998). It is well known that faster depletion of immature thymocytes and T lymphocytes is observed after the appearance of X4 HIV-1 (Berkowitz et al., 1998; Pedroza-Martins et al., 1998; Schnittman et al., 1990). On the contrary, CCR5 is primarily expressed on CD4$^+$ effector memory T lymphocytes (T_{EM}) and macrophages but not on naïve and central memory CD4$^+$ T lymphocytes (T_{CM}) (Sallusto, Geginat, and Lanzavecchia, 2004). Therefore, the selective infection of T_{EM} is thought to leave naïve T lymphocytes and T_{CM} intact. Depletion of T_{EM} by R5 virus has been studied in SIV-infected rhesus macaques (Brenchley et al., 2004; Li et al., 2005). In 14–28 days following infection, the population of extra-lymphoid CCR5$^+$ T_{EM} was depleted up to 90% (Centlivre et al., 2007; Mattapallil et al., 2005; Okoye et al., 2007). At

* Corresponding author. Fax: +81 75 751 4812.
E-mail address: ykoyanag@virus.kyoto-u.ac.jp (Y. Koyanagi).
[1] These authors contributed equally to this study.

0042-6822/$ – see front matter © 2009 Elsevier Inc. All rights reserved.
doi:10.1016/j.virol.2009.08.011

the same time, an obvious reduction in $CD4^+$ T lymphocytes was not found in the PB. In an attempt to compensate for the loss of $CCR5^+$ T_{EM}, $CCR5^-$ T_{CM} was persistently activated and divided in order to prevent the collapse of the T_{EM} compartment (Brenchley, Price, and Douek, 2006). However, $CCR5^-$ T_{CM} lose their regenerative capability after prolonged period of proliferation, leading to decrease in both T_{CM} and T_{EM} compartments (Brenchley, Price, and Douek, 2006). This continuous shortage in $CCR5^+$ T_{EM} and accompanying $CCR5^-$ T_{CM} exhaustion are thought to play an important role in the progression to AIDS (Centlivre et al., 2007). Although the overloading of $CD4^+$ memory T lymphocyte homeostasis serves a compelling model of immunodeficiency in SIV infection, its relevance in HIV-1 infection is still poorly defined. Therefore, it is necessary that memory T lymphocyte infection is studied in an experimental animal model reconstituted with competent human immune cells.

To investigate the dynamics of $CD4^+$ T lymphocyte depletion following HIV-1 infection and the status of HIV-1-producing cells *in vivo*, we infected human $CD34^+$ cells-transplanted newborn NOG mice (NOG-hCD34 mice) with HIV-$1_{JR\text{-}CSF}$ (R5 HIV-1) or HIV-$1_{NL4\text{-}3}$ (X4 HIV-1). Our findings indicate that X4 HIV-1 infection can cause the depletion of $CD4^+$ thymocytes which results in the reduction in both naïve and memory T lymphocytes, while R5 HIV-1 infection can selectively deplete memory $CD4^+$ T lymphocytes. Further analyses indicate that R5 HIV-1 preferentially infects $CCR7^-$ T_{EM} and that the infected cells are predominantly activated and in an actively proliferating state. These results suggest that preferential infection in the activated T_{EM} leads to selective depletion of memory $CD4^+$ T lymphocytes in R5 HIV-1-infected patients.

Results

Kinetics of PB $CD4^+$ T lymphocyte depletion in R5 and X4 HIV-1-infected mice

NOG-hCD34 mice were generated by human $CD34^+$ hematopoietic stem cell transplantation into neonatal NOG mice as described previously (Baenziger et al., 2006; Traggiai et al., 2004). A significant level of human leukocytes was maintained in the whole PB of 13–44

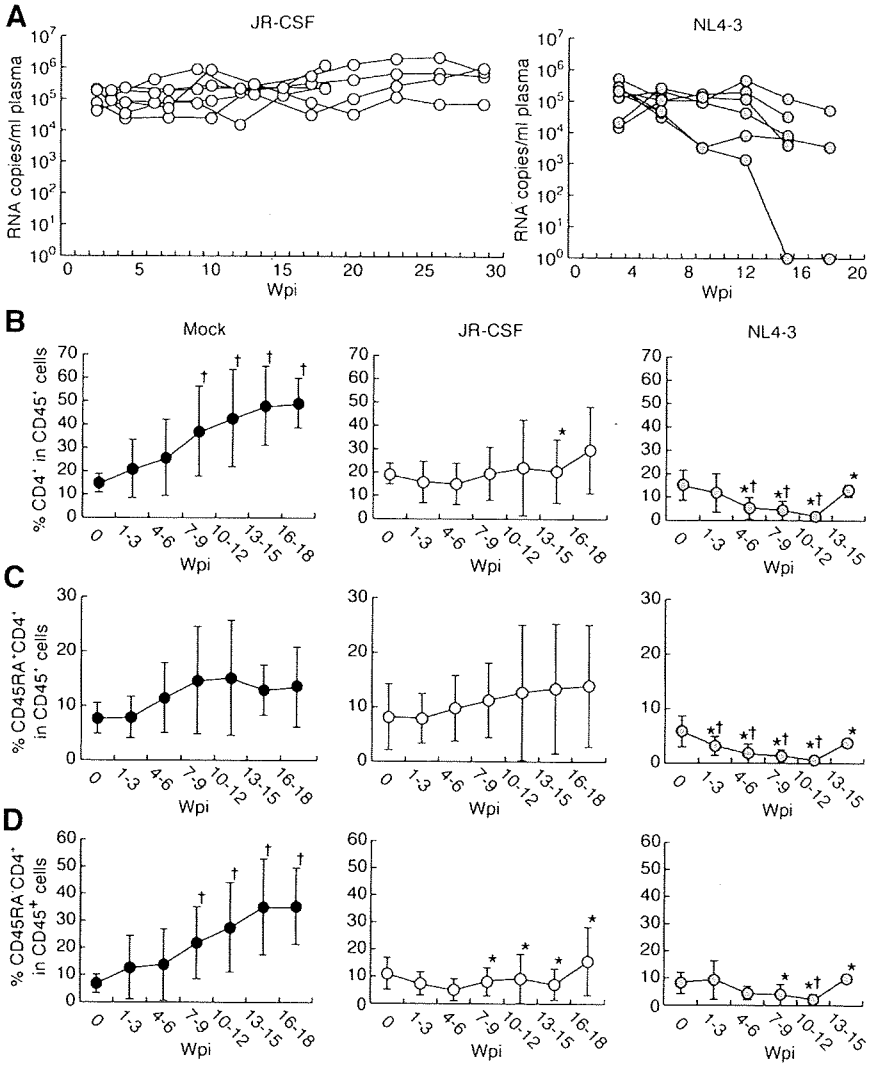

Fig. 1. Longitudinal analysis on plasma viral load and $CD4^+$ T lymphocytes in the PB of R5 and X4 HIV-1-infected mice. NOG-hCD34 mice were intraperitoneally injected with 1×10^5 $TCID_{50}$ of HIV-$1_{JR\text{-}CSF}$ ($n=7$) or HIV-$1_{NL4\text{-}3}$ ($n=8$) between 12 and 13 weeks olds. (A) The longitudinal analysis on the plasma viral load of HIV-$1_{JR\text{-}CSF}$-infected (left) and HIV-$1_{NL4\text{-}3}$-infected (right) mice. (B–D) PB was routinely sampled and analyzed for CD45RA expression in $CD4^+$ T lymphocytes from mock-infected ($n=8$), HIV-$1_{JR\text{-}CSF}$-infected ($n=7$), and HIV-$1_{NL4\text{-}3}$-infected ($n=8$) mice. We assigned data into 7 periodic groups (data taken at 0, between 1–3, 4–6, 7–9, 10–12, 13–15, and 16–18 wpi), and the average percentage and standard deviation were calculated using data obtained from each mouse during each time period. The percentages of $CD4^+$ (B), $CD45RA^+CD4^+$ (C), and $CD45RA^-CD4^+$ (D) T lymphocytes in the peripheral $CD45^+$ cells are shown. Error bars show standard deviations. Daggers represent statistical difference ($P<0.05$) when compared to the value at 0 wpi, and asterisks represent statistical difference when compared to the value obtained from the mock-infected mice.

week old mice (Supplemental Fig. 1A). Hematopoietic and lymphoid organs such as thymus, bone marrow, spleen and lymph nodes were highly repopulated with human mononuclear cells (Supplemental Figs. 1B–E). The expression of CCR5 was mainly restricted within the CD45RA$^-$ memory subset in CD4$^+$ T lymphocytes, and CXCR4 was broadly expressed on both naïve and memory T lymphocytes (Fig. 4C and data not shown) as observed in humans (Ebert and McColl, 2001).

NOG-hCD34 mice were inoculated with either an R5 HIV-1 (HIV-$1_{JR\text{-}CSF}$) or an X4 HIV-1 (HIV-$1_{NL4\text{-}3}$) between 12 and 13 weeks old. HIV-1 RNA was detected in the plasma of these mice as early as 3 weeks post-infection (wpi) and was maintained at high levels (1×10^4 to 10^6 copies per milliliter) until 28 wpi or until sacrificed (Fig. 1A). PB of these mice was then analyzed for longitudinal changes in CD4$^+$ T lymphocytes by flow cytometry. In the PB of both HIV-$1_{JR\text{-}CSF}$-infected and HIV-$1_{NL4\text{-}3}$-infected mice, depletion of human CD4$^+$ T lymphocytes was consistently found (Fig. 1B). In HIV-$1_{NL4\text{-}3}$-infected mice, both CD4$^+$CD45RA$^+$ naïve and CD4$^+$CD45RA$^-$ memory T lymphocytes were depleted, whereas in HIV-$1_{JR\text{-}CSF}$-infected mice, CD4$^+$CD45RA$^-$ memory T lymphocytes were specifically depleted (Figs. 1C and D). These data indicate that the infection with HIV-$1_{NL4\text{-}3}$ caused faster and more severe depletion of both naïve and memory subsets of CD4$^+$ T lymphocytes and the infection with HIV-$1_{JR\text{-}CSF}$ preferentially depleted memory CD4$^+$ T lymphocytes.

Thymopathy in X4 HIV-1-infected mice

To investigate the effect of HIV-1 infection on the thymopoiesis in NOG-hCD34 mice, the thymocytes from HIV-1-infected and mock-infected mice were isolated and were analyzed with flow cytometry. In mock-infected and HIV-$1_{JR\text{-}CSF}$-infected mice, CD4 and CD8 double positive (DP) thymocytes were predominant (Fig. 2A). CD4 single positive (SP) and CD8 SP thymocytes together made up a major fraction of the thymocyte population, and double negative (DN) thymocytes were only a minor fraction. In contrast, thymi from HIV-$1_{NL4\text{-}3}$-infected mice were severely depleted of both CD4 SP thymocytes and DP thymocytes (Figs. 2A–C). Furthermore, thymi from HIV-$1_{NL4\text{-}3}$-infected mice had greatly reduced number of all subsets of thymocytes (Fig. 2D). CD4 SP and DP thymocytes showed the greatest (approximately 100-fold) reduction, while CD8 SP thymocytes showed relatively milder (approximately 10-fold) reduction (Fig. 2D). These data indicate that infection with HIV-$1_{NL4\text{-}3}$ led to disturbed thymopoiesis and that HIV-$1_{JR\text{-}CSF}$ infection did not affect thymopoiesis.

Histological detection of p24-positive cells

HIV-1 p24-positive cells productively produce HIV-1 virions. Since human CD45$^+$ mononuclear cells were very few or absent in HIV-$1_{NL4\text{-}3}$-infected mice when sacrificed, they were not further analyzed (data not shown). As presented in Fig. 3, the immunohistological staining showed the presence of HIV-1 p24-positive cells in all of the bone marrow, spleen, and lymph nodes. HIV-1 p24 staining co-localized with CD4 staining. Also, a larger percentage of cells seemed to be productively infected with HIV-1 in the spleen and lymph nodes.

Depletion of splenic memory CD4$^+$ T lymphocytes

We isolated mononuclear cells from the spleen of HIV-$1_{JR\text{-}CSF}$-infected and mock-infected mice and then analyzed them by flow cytometry. As shown in Fig. 4A, the percentage of CD4$^+$ T lymphocytes in the spleen of HIV-$1_{JR\text{-}CSF}$ mice was smaller than that of mock-infected mice by 2.7-fold ($P=0.003$), showing that HIV-$1_{JR\text{-}CSF}$-infected mice had significantly fewer splenic CD4$^+$ T lymphocytes. Moreover, the percentage of splenic CD4$^+$CD45RA$^-$ memory T lymphocytes in HIV-$1_{JR\text{-}CSF}$-infected mice was smaller than that in the mock-infected mice ($P=0.007$), whereas the percentages of splenic CD4$^+$CD45RA$^+$ naive T lymphocytes were indifferent ($P=0.17$) (Fig. 4B). In mock-infected mice, a significant fraction of CD4$^+$CD45RA$^-$ T lymphocytes were CCR5$^+$ memory T lymphocytes (Fig. 4C). In contrast, in HIV-$1_{JR\text{-}CSF}$-infected mice, we found approximately 20-fold reduction in the percentage (Fig. 4C) and 100-fold reduction in the number of CD4$^+$CD45RA$^-$CCR5$^+$ memory T lymphocytes (data not shown). These results suggest that the CCR5-expressing memory CD4$^+$ T lymphocytes are depleted by direct R5 HIV-1 infection and that such reduction of CCR5-expressing CD4$^+$ T lymphocytes would lead to the decrease in whole memory CD4$^+$ T lymphocytes.

Preferential HIV-1 productive infection in CD4-negative effector memory T lymphocytes

To characterize the immunophenotypes of HIV-1 productively infected cells in NOG-hCD34 mice, splenic mononuclear cells from

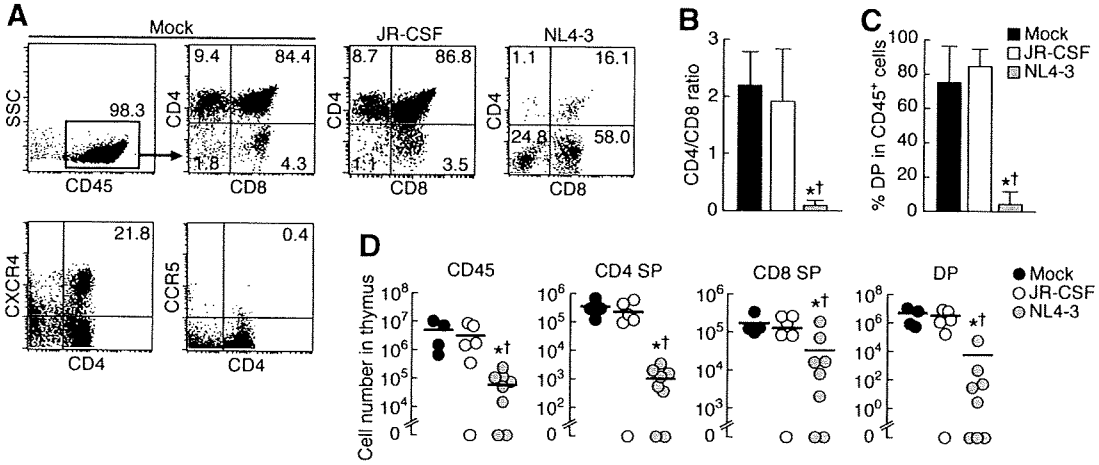

Fig. 2. Thymopathy in X4 HIV-1-infected mice. (A) Representative profile of flow cytometric analysis in thymi of mock-, HIV-$1_{JR\text{-}CSF}$-, and HIV-$1_{NL4\text{-}3}$-infected mice. The numbers in dot plots indicate the percentage of cells in CD45$^+$ thymocytes. (B and C) CD4/CD8 ratio (B) and the percentages of DP cells in CD45$^+$ thymocytes (C) in mock-infected ($n=4$), HIV-$1_{JR\text{-}CSF}$-infected ($n=5$), and HIV-$1_{NL4\text{-}3}$-infected ($n=6$) mice. (D) Number of CD45$^+$, CD4 SP, CD8 SP, and DP cells in thymi of mock-infected ($n=4$), HIV-$1_{JR\text{-}CSF}$-infected ($n=6$), and HIV-$1_{NL4\text{-}3}$-infected ($n=8$) mice. The horizontal bars in D show the average values, and the error bars in B and C show standard deviations. Asterisks indicate statistical significance ($P<0.05$) when compared to mock-infected mice, and daggers indicate statistical significance when compared to HIV-$1_{JR\text{-}CSF}$-infected mice.

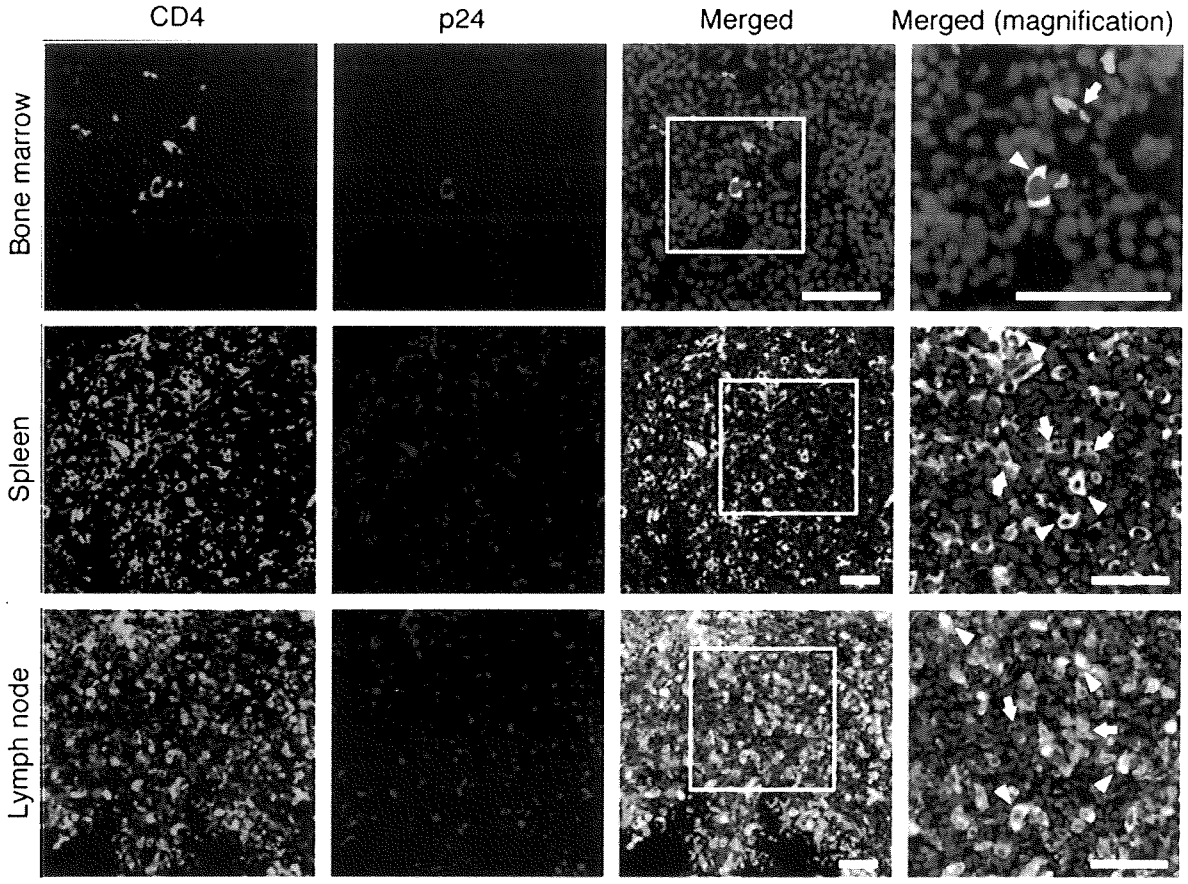

Fig. 3. Histological analysis on R5 HIV-1-infected mice. Representative immunohistological analysis of CD4 (green) and HIV-1 p24 (red) in the slices of bone marrow, spleen, and lymph nodes of HIV-$1_{JR\text{-}CSF}$-infected NOG-hCD34 mice. The low magnification images of the bone marrow slices were taken at ×80, and the high magnification images were taken at ×160. The low magnification images of the spleen and lymph nodes slices were taken at ×40, and the high magnification images were taken at ×80. The areas enclosed with the white squares were enlarged. The arrows point at representative $CD4^+$ cells and the arrowheads point at representative $CD4^+p24^+$ cells. Scale bars, 50 μm.

HIV-$1_{JR\text{-}CSF}$-infected mice were further analyzed for HIV-1 antigen p24 and the expression of lymphocyte surface markers. The anti-p24 antibody that we used did not react with any of the cells isolated from the mock-infected mice (Fig. 5A), as reported previously (Okuma et al., 2008). A significant fraction of splenic leukocytes expressed HIV-1 p24 and thus was productively infected with HIV-1 (Fig. 5A). The productively infected cells expressed surface CD3 but lacked surface CD4 (Figs. 5B and C). On average, over 90% of the $p24^+$ cells were $CD3^+$, yet only about 5% of these cells expressed surface CD4 (Fig. 5C). Also, p24-expressing cells were positive for CD45RO but not for CD45RA, suggesting that they were memory T lymphocytes ($73.7 \pm 24.3\%$ for $CD45RO^+CD45RA^-$ in $p24^+$ cells; Figs. 5D and E). Central memory T lymphocyte (T_{CM}) can be defined as a memory T lymphocyte that expresses CCR7, and effector memory T lymphocyte (T_{EM}) can be defined as a memory T lymphocyte that lacks CCR7 (Sallusto, Geginat, and Lanzavecchia, 2004). In p24-positive cells, $88.0 \pm 3.75\%$ was negative for CCR7 (Figs. 5D and F), suggesting that T_{EM} dominantly and productively infect with HIV-1.

Productive HIV-1 infection in activated and dividing lymphocytes

To investigate the activation status of the productively infected cells, splenic mononuclear cells were stained with anti-p24, anti-Ki67, and anti-CD69 antibodies. Ki67 antigen is exclusively expressed in proliferating cells, and CD69 is expressed on the surface of the activated cells at the early phase (Sereti et al., 2007; Vatakis et al., 2007). In splenic $CD4^+$ T lymphocytes from mock-infected mice or p24-negative splenocytes from HIV-$1_{JR\text{-}CSF}$-infected mice, only a minor fraction of the cells expressed either Ki67 or CD69 (Figs. 6A and B). In contrast, the majority of p24-positive splenocytes from HIV-$1_{JR\text{-}CSF}$-infected mice expressed Ki67 and/or CD69 (Figs. 6A and B). Also, the percentage of cells positive for both Ki67 and CD69 were higher in p24-positive cells than in p24-negative splenocytes from HIV-$1_{JR\text{-}CSF}$-infected mice and in splenic $CD4^+$ T lymphocytes from mock-infected mice (Fig. 6B). These results indicate that a significantly higher frequency of p24-positive cells is activated and/or proliferating cells. Notably, although the frequency was significantly low, we could detect $Ki67^-CD69^-$ resting T lymphocytes in p24-positive cells (Figs. 6A and B).

To further analyze the cell cycle of HIV-1 productively infected cells (i.e., p24-positive cells), we carried out Hoechst staining, which quantifies DNA content of the cells. Ki67 staining in combination with the Hoechst staining will sort cells into those in G_0/G_{1a}, G_{1b}, and $S/G_2/M$ phases of the cell cycle (Wilpshaar et al., 2000). As shown in Fig. 6C, non-stimulated human peripheral blood leukocytes (PBLs) predominantly exist in G_0/G_{1a} phases ($Ki67^-Hoechst^{low}$, lower left in the quadrant), while PHA-activated human PBLs predominantly exist in cycling G_{1b} phase ($Ki67^+Hoechst^{low}$, upper left in the quadrant) and $S/G_2/M$ phases ($Ki67^+Hoechst^{high}$, upper right in the quadrant). By using this method, we observed that p24-positive cells contained a significantly higher frequency of cells in the G_{1b} phase. In addition, the percentage of p24-positive cells in $S/G_2/M$ phases was significantly higher than $CD4^+$ splenocytes from mock-infected mice (Figs. 6D and E). These findings indicate that the majority of HIV-1-producing cells in the spleen of R5 HIV-1-infected mice are activated and in cycling phase. On the other hand, we detected the p24-

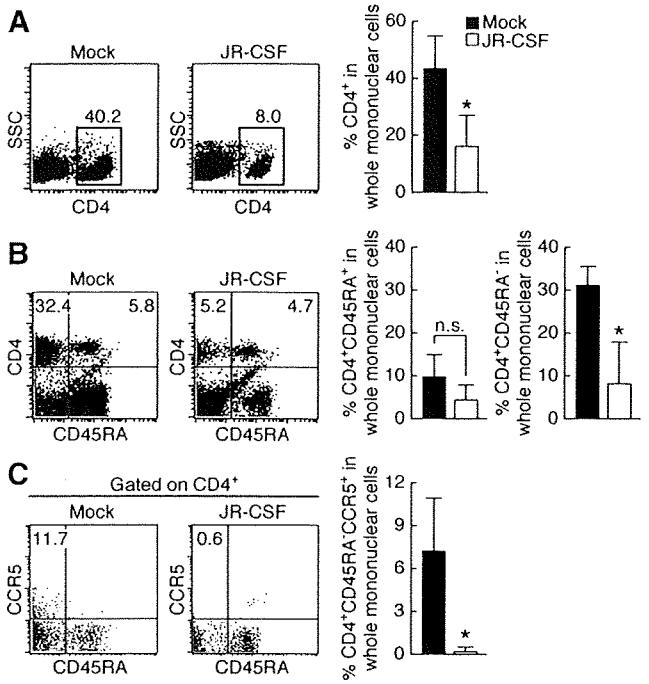

Fig. 4. The effect of R5 HIV-1 infection on the splenic $CD4^+$ T lymphocyte population. (A–C) Staining of splenic nucleated cells from the spleen of mock-infected ($n=4$) and HIV-$1_{JR\text{-}CSF}$-infected ($n=4$) mice were stained with CD4 (A), CD4 and CD45RA (B), and CCR5, CD4, and CD45RA (C). Representative profiles are shown, and the numbers in dot plots indicate the percentage of cells in $CD45^+$ splenic human leukocytes (A and B) or in $CD4^+$ cells (C). The graphs show the percentages of cells possessing each phenotype in whole mononuclear cells. The error bars show standard deviations. Asterisks indicate statistical significance ($P<0.05$) when compared to mock-infected mice.

positive splenocytes in G_0/G_{1a} phases, although the frequency was significantly lower than p24-negative splenocytes or $CD4^+$ splenocytes from mock-infected mice (Figs. 6D and E). These data suggest that a fraction of resting cells productively infects HIV-1. Moreover, we detected the significantly higher percentage of cells in $S/G_2/M$ phases in splenic p24-negative cells of HIV-$1_{JR\text{-}CSF}$-infected mice when comparing to that in splenic $CD4^+$ T lymphocytes of mock-infected mice (Figs. 6D and E).

Discussion

To investigate the mechanisms of $CD4^+$ T lymphocyte depletion by HIV-1 infection, we utilize human $CD34^+$ cells-transplanted NOG mice (Ito et al., 2002) and demonstrate that human $CD4^+$ T lymphocytes were differentially affected by X4 and R5 HIV-1 infection (Figs. 1–4). X4 virus induced immediate depletion of both naïve and memory $CD4^+$ T lymphocytes in periphery, while R5 virus gradually depleted memory $CD4^+$ T lymphocytes in the PB (Fig. 1) and spleen (Fig. 4). Our data suggest that distinctive pathogenesis of X4 and R5 viruses in NOG-hCD34 mice was caused by thymopathy (Fig. 2) and preferential infection of activated and dividing T_{EM} (Figs. 5 and 6), respectively. This is the first report addressing the mechanisms and dynamics of HIV-1-induced $CD4^+$ T lymphocyte depletion *in vivo*.

As previously shown in X4 SHIV-infected macaques (Ho et al., 2005; Nishimura et al., 2004), we observed the drastic loss of both naïve and memory T lymphocytes by X4 HIV-1-infected NOG-hCD34 mice (Fig. 1). We also found that $CD4^+$ thymocytes in NOG-hCD34 mice abundantly express CXCR4 (Fig. 2A) and that the $CD4^+$ thymocytes including DP and CD4 SP were preferentially reduced in HIV-$1_{NL4\text{-}3}$-infected mice (Fig. 2). It has been reported that intrathymic infection by X4 HIV-1 can lead to severe T lymphocytopenia (Berkowitz et al., 1998; Schnittman et al., 1990; Ye, Kirschner, and Kourtis, 2004). Therefore, our results suggest that the primary mechanism for naïve and memory T lymphocyte depletion in X4 virus infection can be attributed to impaired thymopoiesis caused by intrathymic infection.

In contrast to X4 HIV-1 infection, the depletion of PB $CD4^+$ T lymphocytes was more gradual and less intense in R5 HIV-1 infection and was confined to $CD45RA^-$ memory $CD4^+$ T lymphocytes (Fig. 1D). The selective depletion of memory $CD4^+$ T lymphocytes by R5 infection was also found in the spleen (Fig. 4). On the other hand, thymopathy was not detected in HIV-$1_{JR\text{-}CSF}$-infected mice (Fig. 2). These findings suggest that the selective depletion of memory $CD4^+$ T lymphocytes in PB and spleen of HIV-$1_{JR\text{-}CSF}$-infected mice caused through a different mechanism from HIV-$1_{NL4\text{-}3}$, and the mechanisms are further discussed below.

To investigate the mechanisms of memory $CD4^+$ T lymphocyte depletion in R5 HIV-1 infection in-depth, a series of flow cytometric analyses was carried out. The majority of $p24^+$ productively infected cells in the spleen were $CD3^+$ T lymphocytes (Figs. 5B and C). However, these infected cells were negative for surface CD4 (Figs. 5B

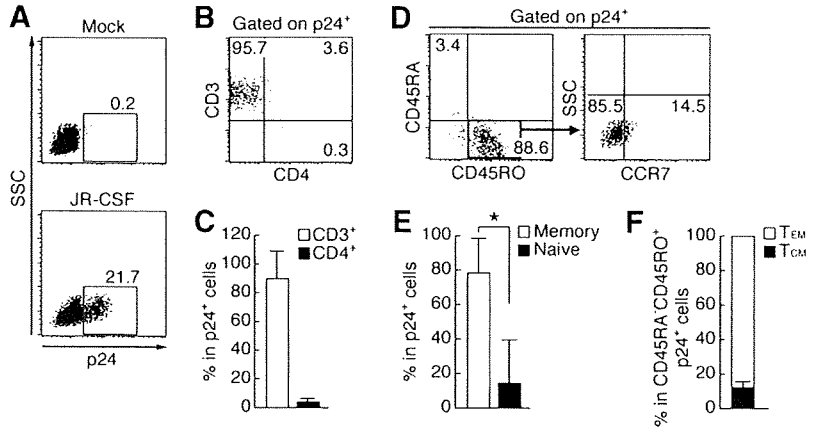

Fig. 5. Phenotype of productively infected $p24^+$ cells in the spleen of R5 HIV-1-infected mice. (A) Representative profiles of flow cytometric p24 staining in splenic nucleated cells of mock-infected ($n=4$) and HIV-$1_{JR\text{-}CSF}$-infected ($n=6$) mice. The numbers indicate the percentage of cells in splenic nucleated cells. (B and C) Staining of splenic nucleated cells of HIV-$1_{JR\text{-}CSF}$-infected mice for p24, CD3, and CD4. Representative profiles are shown in B, and the numbers in each quadrant indicate the percentage of cells in $p24^+$ cells. The percentages of each population in $p24^+$ cells are shown in C. (D–F) Staining of splenic nucleated cells of HIV-$1_{JR\text{-}CSF}$-infected mice for p24, CD45RA, CD45RO, and CCR7. Representative profiles are shown in D, and the numbers in each quadrant indicate the percentage of cells in $p24^+$ cells (left) or in $p24^+CD45RA^-CD45RO^+$ cells (right). The percentages of memory ($CD45RA^-CD45RO^+$) and naïve ($CD45RA^+CD45RO^-$) phenotyped cells in $p24^+$ cells are shown in E. The percentages of T_{EM} ($CCR7^-CD45RA^-CD45RO^+$) and T_{CM} ($CCR7^+CD45RA^-CD45RO^+$) in $p24^+$ cells are shown in F. The error bars in C, E, and F show standard deviations. Asterisks indicate statistical significance ($P<0.05$).

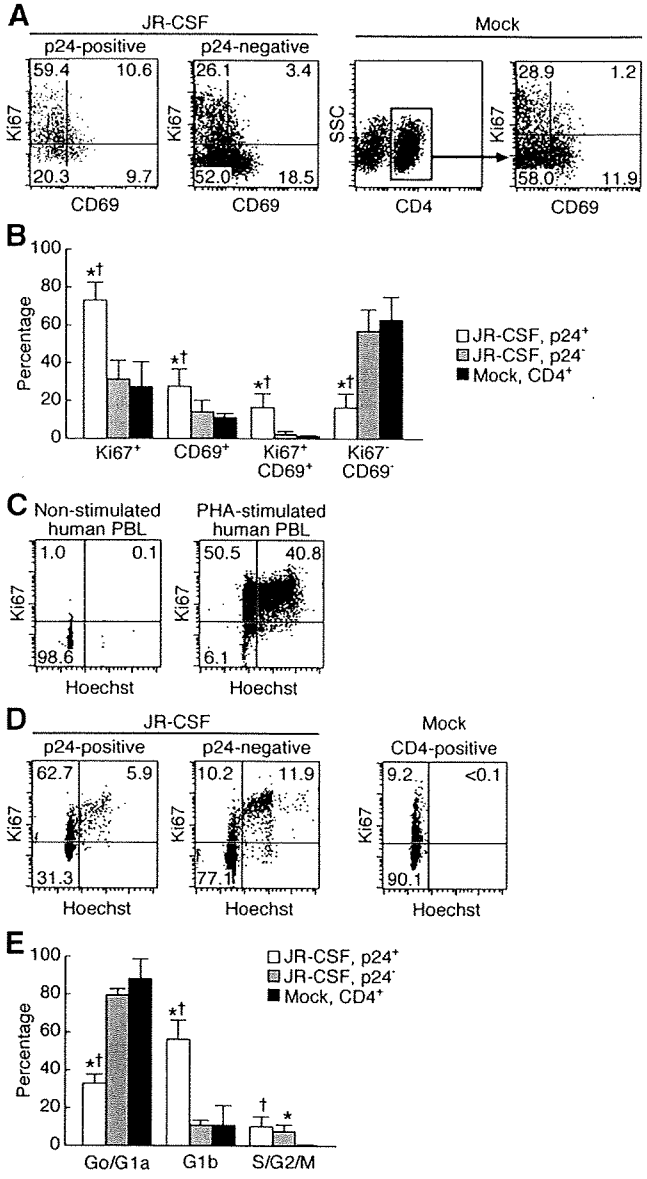

Fig. 6. Cell cycle analyses on productively infected p24$^+$ cells in the spleen of R5 HIV-1-infected mice. (A and B) Staining of splenic nucleated cells of mock-infected ($n=3$) and HIV-$1_{JR\text{-}CSF}$-infected ($n=4$) mice for Ki67, CD69, and either CD4 or p24. Representative profiles are shown in A, and each number indicates the percentage of cells in each quadrant. The graph in B shows the average percentages of cells possessing each population. (C) A representative profile of cell cycle analysis on non-stimulated human PBL (left panel) and PHA-activated human PBL (right panel) by using anti-Ki67 antibody and Hoechst. Each number indicates the percentage of cells in each quadrant. Ki67$^-$Hoechst^{low} (lower left in quadrant) indicates G_0/G_{1a} phase, while Ki67$^+$Hoechst^{low} (upper left in quadrant) and Ki67$^+$Hoechst^{high} (upper right in quadrant) indicate G_{1b} and $S/G_2/M$ phases, respectively. (D and E) Staining of splenic nucleated cells of mock-infected mice ($n=4$) for CD4, Ki67, and Hoechst, and HIV-$1_{JR\text{-}CSF}$-infected mice ($n=4$) for p24, Ki67, and Hoechst. Representative profiles are shown in D, and each number indicates the percentage of cells in each quadrant. The graph in E shows the average percentages of cells in each population. The error bars in B and E show standard deviations. Asterisks indicate statistical significance ($P<0.05$) when compared to the value of p24-negative cells in HIV-$1_{JR\text{-}CSF}$-infected mice, and daggers indicate statistical significance when compared to the value of CD4-positive cells in mock-infected mice.

and C), although immunohistological analysis revealed that splenic p24$^+$ cells expressed CD4 molecules (Fig. 3). These results suggest that surface CD4 molecules are severely down-regulated following infection. In fact, it has been well documented that HIV-1 gene products such as *Nef* (Fackler, Alcover, and Schwartz, 2007; Roeth and Collins, 2006), *Env* (Crise, Buonocore, and Rose, 1990), and *Vpu* (Bour and Strebel, 2003; Geleziunas, Bour, and Wainberg, 1994) have the potential to down-regulate CD4 molecules from the surface of infected cells (Lindwasser, Chaudhuri, and Bonifacino, 2007). Similar down-regulation of surface CD4 has also been reported in lymph nodes and PB of HIV-1-infected patients (Cheney et al., 2006; Kaiser et al., 2007; Marodon et al., 1999). Therefore, this down-regulation of surface CD4 molecules in HIV-$1_{JR\text{-}CSF}$-infected mice is physiologically relevant and can play a role in the reduction of CD4$^+$ T lymphocytes.

In HIV-$1_{JR\text{-}CSF}$-infected mice, more than 80% of the productively infected cells were activated and in cycling phase (Fig. 6). It has been well known that activated cells massively produce HIV-1 virions (Ho et al., 1995). Therefore, this result suggests that the persistent viremia in R5 infection (Fig. 1A) is primarily due to the productive infection in the activated and proliferating cells. On the other hand, a fraction of infected cells were quiescent T lymphocytes negative for both activation and proliferation markers (Fig. 6). It is thought that HIV-1 cannot manifest productive infection in quiescent cells (Stevenson et al., 1990; Zack et al., 1990). However, studies on *ex vivo* infected human tonsil histocultures (Eckstein et al., 2001; Kinter et al., 2003), small intestines and cervix of SIV-infected rhesus macaques (Li et al., 2005; Zhang et al., 1999; Zhang et al., 2004), and HIV-1-infected patients (Zhang et al., 1999) have established that quiescent T lymphocytes residing in the lymphoid tissues are capable of supporting productive SIV or HIV-1 infection. Our results provide further support that productive infection of HIV-1 can take place in non-dividing cells, presumably resting T lymphocytes, in NOG-hCD34 mice. Productive infection not only in proliferative cells but also in quiescent cells may be an important factor in CD4$^+$ T lymphocyte depletion and persistent virus infection.

The preferential infection of CD45RO$^+$CD45RA$^-$ memory T lymphocytes with R5 HIV-1 is also the evidence supportive for the selective depletion of memory CD4$^+$ T lymphocytes (Figs. 5D and E). Nevertheless, only 16.3 ± 9.7% of splenic CD4$^+$ T lymphocytes expressed CCR5 in NOG-hCD34 mice, and the severe depletion of memory T lymphocytes in R5 HIV-1 infection cannot be explained by cell death caused by infection solely. In this regard, it has been reported that memory CD4$^+$ T lymphocyte reduction in SIV-infected macaques can be initiated by specific disruption of T_{EM} due to its preferential infection in the acute phase (Centlivre et al., 2007; Mattapallil et al., 2005; Okoye et al., 2007). In response to the T_{EM} reduction, T_{CM} proliferates and supplies *de novo* T_{EM} (Sallusto, Geginat, and Lanzavecchia, 2004). However, Brenchley et al. (2004) and Okoye et al. (2007) have reported that R5 virus infection induces chronic immune activation in macaques, which leads to the attenuation of regenerative capacity of T_{CM} (Brenchley et al., 2004; Okoye et al., 2007). In addition to the depletion of T_{EM} by direct infection, the attenuation of regenerative potential of T_{CM} causes not only the loss of T_{CM} but also the shortage of T_{EM} and eventually leads to the reduction of whole memory T lymphocytes (Brenchley et al., 2004; Okoye et al., 2007). This hypothesis of the dynamics of CD4$^+$ T lymphocyte depletion has been helpful for explaining the memory CD4$^+$ T lymphocyte in effector sites of SIV-infected macaques. Our observations in HIV-$1_{JR\text{-}CSF}$-infected mice, the severe depletion of memory T lymphocytes despite the limited availability of CCR5-expressing CD4$^+$ T lymphocytes and the preferential infection in T_{EM}, can be explained by the aforementioned hypothesis proposed in the previous literature (Brenchley et al., 2004; Okoye et al., 2007). Notably, we found that the frequency of cells in $S/G_2/M$ phases elevated in splenic p24-negative cells of HIV-$1_{JR\text{-}CSF}$-infected mice when comparing to that in splenic CD4$^+$ T lymphocytes of mock-infected mice (Figs. 6D and E). These data may explain that HIV-1 pathophysiology is caused by accelerated cells division, ultimately leading to the exhaustion of CD4$^+$ T lymphocytes. Taken together, our findings suggest that the selective infection of T_{EM} may be an important event that governs CD4$^+$ T lymphocyte depletion not

only in the effector sites of macaques during SIV infection but also in lymphoid organs during HIV-1 infection.

In summary, we showed differential $CD4^+$ T lymphocyte reduction in R5 and X4 HIV-1 infection. We report for the first time the selective depletion of memory $CD4^+$ T lymphocytes and the preferential infection of T_{EM} in an experimental model of R5 HIV-1 infection. Our data suggest that HIV-1 infection in T_{EM} can be an important step leading to $CD4^+$ T lymphocyte decline. Our findings confirm the applicability of NOG-hCD34 mice as a useful model to study the dynamics of HIV-1 pathogenesis including $CD4^+$ T lymphocytes depletion *in vivo*.

Materials and methods

Mice

NOD/SCID/IL-2Rγ^{null} (NOG) mice (Ito et al., 2002) were obtained from the Central Institute for Experimental Animals (Kanagawa, Japan). The mice were maintained under specific pathogen-free conditions and were handled in accordance with the Regulation on Animal Experimentation at Kyoto University.

Purification and transplantation of cord blood-derived CD34 cells

The purification of cord blood-derived CD34 cells was conducted as described previously (Ishikawa et al., 2005; Ito et al., 2002). Fresh human cord blood was obtained with parent written informed consent from healthy full-term newborns and CD34 MicroBead Kit (Miltenyi Biotec Inc, Auburn, CA) was used to isolate $hCD34^+$ cells according to the manufacturer's instructions. Cells were either stored at −80 °C or immediately transplanted when newborn mice were available. $CD34^+$ cells ($5–12 \times 10^4$) were intrahepatically injected into newborn mice of ages between 0 and 2 days after total radiation of 10 cGy per mouse in MBR-1520 x-ray irradiator (Hitachi Medico, Tokyo, Japan).

Peripheral blood collection and isolation of nucleated cells from organs

PB was routinely taken from NOG-hCD34 mice under ether anesthesia via retro-orbital venousplexus as described previously (Ishikawa et al., 2005). The red blood cells in the PB were lysed in preparation for flow cytometric analysis in 1× BD lysis buffer (BD Pharmingen, San Diego, CA). When the mice were sacrificed, PB was taken by cardiac puncture. Lymph nodes, thymi, spleen, and bone marrow were taken from HIV-1-infected and mock-infected mice upon sacrifice for histological or flow cytometric analysis. Lymph nodes and thymi were gently homogenized using a homogenizer pestle and spleens were crushed and rubbed on a steal mesh with 1-mm grids to generate single cell suspensions in RPMI 1640 supplemented with 4% fetal calf serum (FCS). To collect bone marrow, thigh bones were dissected at both ends and the interior was flushed with RPMI 1640 supplemented with 4% FCS. The cells were immediately used for flow cytometric analysis or stored in Cell Banker (Juji Field Inc., Tokyo, Japan) at −80 °C until use. As there are some variations in the combination of antibodies used to study the human cell population in each mouse, the number of data collected for each surface marker may differ. Data used for any longitudinal analysis were taken from identical mice.

Flow cytometric analysis of human blood cells in transplanted mice

The staining for flow cytometric analysis was done with some modifications to the protocol previously described (Sato et al., 2008). Briefly, for the surface staining, the cells were blocked with FcR blocker (Miltenyi Biotec Inc) for 5 min at room temperature (RT) and then incubated with the appropriate antibodies at optimum concentration in 1× phosphate-buffered saline (PBS) containing 2% FCS for 30 min at 4 °C. Fluorescein isothiocyanate-conjugated (FITC-conjugated) anti-human CD19 (HD37; Dako, Tokyo, Japan), CD8 (DK25; Dako), CD14 (TUK4; Miltenyi Biotec Inc), CD4 (L3T4; eBioscience, San Diego, CA), CD3 (UCHT1; BD Pharmingen, San Diego, CA), CCR5 (3A9; BD Pharmingen), and CD303/BDCA2 (AC144; Miltenyi Biotec Inc) mouse IgG monoclonal antibodies (mAb); phycoerythrin-conjugated anti-human CD3 (UCHT1; Dako), CD4 (MT310; Dako), CD34 (AC136; Miltenyi Biotec Inc), CD11c (B-ly6; BD Pharmingen), CXCR4 (12G5; BD Pharmingen), CCR7 (FAB197; R&D systems, Abingdon, UK), and CCR5 (3A9; BD Pharmingen) mouse IgG mAb; biotinylated anti-human CD45 (H130; eBioscience), CD45RA (HI-100; BD Pharmingen), CD8 (RPA-T8; BD Pharmingen), CD4 (RPA-T4; BD Pharmingen), and mouse IgG mAb; peridinin-chlorophyll-conjugated (PerCP-conjugated) anti-human CD69 (L78; BD Immunocytometry Systems, San Jose, CA) mouse IgG mAb; PE-Cy5-conjugated anti-human HLA-DR (G46-6; BD Pharmingen) mouse IgG mAb; allophycocyamin-conjugated anti-human CD45RO (UCHL1; BD Pharmingen) and CD8 (DK25; Dako) mouse IgG mAb were used. Each antibody was controlled with appropriate isotype antibodies purchased from Dako and BD Pharmingen. Streptavidin-PerCP (SA-PerCP) was purchased from BD Immunocytometry Systems. Following the incubation, the cells were washed and further incubated with SA-PerCP for 30 min at 4 °C, if needed. For the intracellular staining, the cells were permeabilized and fixed by treatment with BD Cytoperm/Cytofix solution (BD Pharmingen) and were stained with FITC-conjugated anti-HIV-1 p24 (clone 2C2) (Okuma et al., 2008) and anti-human Ki67 (B56; BD Pharmingen) mouse IgG mAb for 30 min at 4°C in 1× BD PermWash buffer (BD Pharmingen). For DNA staining to analyze cell cycle, the cells were incubated with Hoechst33342 (Invitrogen, Carlsbad, CA) for 30 min at 4 °C as described previously (Wilpshaar et al., 2000). Data collection was performed on BD FACSCan (BD Biosciences) for 3-color staining, BD FACSCalibur (BD Biosciences) for 4-color staining, and BD FACSCanto (BD Biosciences) for cell cycle analyses using Hoechst33342, and the obtained data were analyzed with CellQuest software (BD Immunocytometry System, San Jose, CA).

HIV-1 infection

NOG mice were injected intraperitoneally with RPMI 1640 ($n=8$) or 1×10^5 50% tissue culture infective doses ($TCID_{50}$) of $HIV\text{-}1_{JR\text{-}CSF}$ ($n=7$) or $HIV\text{-}1_{NL4\text{-}3}$ ($n=8$) between 12 and 13 weeks of ages. The viruses used were prepared by transfection as previously described (Sato et al., 2008). Infectious titers in the form of $TCID_{50}$ of each virus stock were determined by endpoint dilution with phytohemagglutinin-activated PBMCs as described (Koyanagi et al., 1997).

Detection of HIV-1 RNA in the plasma of infected mice

The detection of HIV-1 RNA in the plasma of the infected mice was routinely carried out using Amplicor HIV-1 monitor v1.5 according to the manufacturer's protocol (Roche Diagnostics, Mannheim, Germany).

Immunohistological analysis

Organs were fixed in 1× PBS containing 4% paraformalhyde and embedded in OCT compound (Sakura Finetechnical, Tokyo, Japan) after immersion in 10%–20% gradient sucrose. The OCT embedded organs were then sliced and were permeabilized with 0.1% Triton-X at RT for 10 min, incubated three times with 10 mM glycine for 5 min and blocked with 5% normal goat serum at RT for 1 hr. The sections were then incubated with mouse anti-HIV-1 p24 (Kal-1; Dako) IgG mAb at 4°C overnight, followed by incubation with Alexa Fluor 488-conjugated goat anti-mouse IgG (Invitrogen) at RT for 2 hr. The sections were further incubated with biotinylated mouse anti-

human CD4 IgG mAb (RFT-4g; Southern Biotech, Birmingham, AL) at 4°C overnight, followed by incubation with Streptavidin–Alexa Fluor 647 (Invitrogen) and Hoeschst33342 at RT for 2 hr. All the antibody staining was performed in blocking solution. Images were acquired with a Leica TCS SP2 AOBS confocal laser microscope (Leica Microsystems, Heidelberg, Germany).

Statistical analysis

Data were expressed as an average with standard deviation. Significant differences between data groups were determined by Student's *t* test or paired *t* test. A *P* value less than 0.05 was considered significantly different.

Acknowledgments

We would like to thank Peter Gee (Institute for Virus Research, Kyoto University) for proofreading of our manuscript and Munetada Haruyama (the Department of Pediatrics, Kyoto University) for their generous help in our study. We also would like to express our appreciation for Ms. Kotubu Misawa's dedicated support. This work was supported by a Grant-in-Aid for Scientific Research on Priority Areas from the Ministry of Education, Culture, Sports, Sciences, and Technology of Japan; a Health and Labour Science Research Grant (Research on Publicly Essential Drugs and Medical Devices) from the Ministry of Health, Labor and Welfare of Japan; and Japan Human Science Foundation. K.S. was supported by Research Fellowships of the Japan Society for the Promotion of Science for Young Scientists. Y. K. was supported by a grant from the Naito Foundation.

Appendix A. Supplementary data

Supplementary data associated with this article can be found, in the online version, at doi:10.1016/j.virol.2009.08.011.

References

Ambrose, Z., KewalRamani, V.N., Bieniasz, P.D., Hatziioannou, T., 2007. HIV/AIDS: in search of an animal model. Trends Biotechnol. 25, 333–337.

Baenziger, S., Tussiwand, R., Schlaepfer, E., Mazzucchelli, L., Heikenwalder, M., Kurrer, M.O., Behnke, S., Frey, J., Oxenius, A., Joller, H., Aguzzi, A., Manz, M.G., Speck, R.F., 2006. Disseminated and sustained HIV infection in $CD34^+$ cord blood cell-transplanted $Rag2^{-/-}\gamma_c^{-/-}$ mice. Proc. Natl. Acad. Sci. U. S. A. 103, 15951–15956.

Berger, E.A., Murphy, P.M., Farber, J.M., 1999. Chemokine receptors as HIV-1 coreceptors: roles in viral entry, tropism, and disease. Annu. Rev. Immunol. 17, 657–700.

Berkowitz, R.D., Alexander, S., Bare, C., Linquist-Stepps, V., Bogan, M., Moreno, M.E., Gibson, L., Wieder, E.D., Kosek, J., Stoddart, C.A., McCune, J.M., 1998. CCR5- and CXCR4-utilizing strains of human immunodeficiency virus type 1 exhibit differential tropism and pathogenesis *in vivo*. J. Virol. 72, 10108–10117.

Bour, S., Strebel, K., 2003. The HIV-1 Vpu protein: a multifunctional enhancer of viral particle release. Microbes. Infect. 5, 1029–1039.

Brenchley, J.M., Price, D.A., Douek, D.C., 2006. HIV disease: fallout from a mucosal catastrophe? Nat. Immunol. 7, 235–239.

Brenchley, J.M., Schacker, T.W., Ruff, L.E., Price, D.A., Taylor, J.H., Beilman, G.J., Nguyen, P.L., Khoruts, A., Larson, M., Haase, A.T., Douek, D.C., 2004. $CD4^+$ T cell depletion during all stages of HIV disease occurs predominantly in the gastrointestinal tract. J. Exp. Med. 200, 749–759.

Centlivre, M., Sala, M., Wain-Hobson, S., Berkhout, B., 2007. In HIV-1 pathogenesis the die is cast during primary infection. AIDS 21, 1–11.

Cheney, K.M., Kumar, R., Purins, A., Mundy, L., Ferguson, W., Shaw, D., Burrell, C.J., Li, P., 2006. HIV type 1 persistence in $CD4^-/CD8^-$ double negative T cells from patients on antiretroviral therapy. AIDS Res. Hum. Retroviruses 22, 66–75.

Crise, B., Buonocore, L., Rose, J.K., 1990. CD4 is retained in the endoplasmic reticulum by the human immunodeficiency virus type 1 glycoprotein precursor. J. Virol. 64, 5585–5593.

Ebert, L.M., McColl, S.R., 2001. Coregulation of CXC chemokine receptor and CD4 expression on T lymphocytes during allogeneic activation. J. Immunol. 166, 4870–4878.

Eckstein, D.A., Penn, M.L., Korin, Y.D., Scripture-Adams, D.D., Zack, J.A., Kreisberg, J.F., Roederer, M., Sherman, M.P., Chin, P.S., Goldsmith, M.A., 2001. HIV-1 actively replicates in naive $CD4^+$ T cells residing within human lymphoid tissues. Immunity 15, 671–682.

Fackler, O.T., Alcover, A., Schwartz, O., 2007. Modulation of the immunological synapse: a key to HIV-1 pathogenesis? Nat. Rev. Immunol. 7, 310–317.

Geleziunas, R., Bour, S., Wainberg, M.A., 1994. Cell surface down-modulation of CD4 after infection by HIV-1. FASEB J. 8, 593–600.

Ho, D.D., Neumann, A.U., Perelson, A.S., Chen, W., Leonard, J.M., Markowitz, M., 1995. Rapid turnover of plasma virions and CD4 lymphocytes in HIV-1 infection. Nature 373, 123–126.

Ho, S.H., Shek, L., Gettie, A., Blanchard, J., Cheng-Mayer, C., 2005. V3 loop-determined coreceptor preference dictates the dynamics of $CD4^+$-T-cell loss in simian–human immunodeficiency virus-infected macaques. J. Virol. 79, 12296–12303.

Ishikawa, F., Yasukawa, M., Lyons, B., Yoshida, S., Miyamoto, T., Yoshimoto, G., Watanabe, T., Akashi, K., Shultz, L.D., Harada, M., 2005. Development of functional human blood and immune systems in NOD/SCID/IL2 receptor γ $chain^{null}$ mice. Blood 106, 1565–1573.

Ito, M., Hiramatsu, H., Kobayashi, K., Suzue, K., Kawahata, M., Hioki, K., Ueyama, Y., Koyanagi, Y., Sugamura, K., Tsuji, K., Heike, T., Nakahata, T., 2002. NOD/SCID/γ_c^{null} mouse: an excellent recipient mouse model for engraftment of human cells. Blood 100, 3175–3182.

Kaiser, P., Joos, B., Niederost, B., Weber, R., Gunthard, H.F., Fischer, M., 2007. Productive human immunodeficiency virus type 1 infection in peripheral blood predominantly takes place in CD4/CD8 double-negative T lymphocytes. J. Virol. 81, 9693–9706.

Kinter, A., Moorthy, A., Jackson, R., Fauci, A.S., 2003. Productive HIV infection of resting $CD4^+$ T cells: role of lymphoid tissue microenvironment and effect of immunomodulating agents. AIDS Res. Hum. Retroviruses 19, 847–856.

Koyanagi, Y., Tanaka, Y., Ito, M., Yamamoto, N., 2008. Humanized mice for human retrovirus infection. Curr. Top Microbiol. Immunol. 324, 133–148.

Koyanagi, Y., Tanaka, Y., Kira, J., Ito, M., Hioki, K., Misawa, N., Kawano, Y., Yamasaki, K., Tanaka, R., Suzuki, Y., Ueyama, Y., Terada, E., Tanaka, T., Miyasaka, M., Kobayashi, T., Kumazawa, Y., Yamamoto, N., 1997. Primary human immunodeficiency virus type 1 viremia and central nervous system invasion in a novel hu-PBL-immunodeficient mouse strain. J. Virol. 71, 2417–2424.

Li, Q., Duan, L., Estes, J.D., Ma, Z.M., Rourke, T., Wang, Y., Reilly, C., Carlis, J., Miller, C.J., Haase, A.T., 2005. Peak SIV replication in resting memory $CD4^+$ T cells depletes gut lamina propria $CD4^+$ T cells. Nature 434, 1148–1152.

Lindwasser, O.W., Chaudhuri, R., Bonifacino, J.S., 2007. Mechanisms of CD4 downregulation by the Nef and Vpu proteins of primate immunodeficiency viruses. Curr. Mol. Med. 7, 171–184.

Lusso, P., 2006. HIV and the chemokine system: 10 years later. EMBO J. 25, 447–456.

Marodon, G., Warren, D., Filomio, M.C., Posnett, D.N., 1999. Productive infection of double-negative T cells with HIV *in vivo*. Proc. Natl. Acad. Sci. U. S. A. 96, 11958–11963.

Mattapallil, J.J., Douek, D.C., Hill, B., Nishimura, Y., Martin, M., Roederer, M., 2005. Massive infection and loss of memory $CD4^+$ T cells in multiple tissues during acute SIV infection. Nature 434, 1093–1097.

McCune, J.M., 2001. The dynamics of $CD4^+$ T-cell depletion in HIV disease. Nature 410, 974–979.

Moore, J.P., Kitchen, S.G., Pugach, P., Zack, J.A., 2004. The CCR5 and CXCR4 coreceptors – central to understanding the transmission and pathogenesis of human immunodeficiency virus type 1 infection. AIDS Res. Hum. Retroviruses 20, 111–126.

Nishimura, Y., Igarashi, T., Donau, O.K., Buckler-White, A., Buckler, C., Lafont, B.A., Goeken, R.M., Goldstein, S., Hirsch, V.M., Martin, M.A., 2004. Highly pathogenic SHIVs and SIVs target different $CD4^+$ T cell subsets in rhesus monkeys, explaining their divergent clinical courses. Proc. Natl. Acad. Sci. U. S. A. 101, 12324–12329.

O'Brien, W.A., Hartigan, P.M., Martin, D., Esinhart, J., Hill, A., Benoit, S., Rubin, M., Simberkoff, M.S., Hamilton, J.D., 1996. Changes in plasma HIV-1 RNA and $CD4^+$ lymphocyte counts and the risk of progression to AIDS. Veterans Affairs Cooperative Study Group on AIDS. N. Engl. J. Med. 334, 426–431.

Okoye, A., Meier-Schellersheim, M., Brenchley, J.M., Hagen, S.I., Walker, J.M., Rohankhedkar, M., Lum, R., Edgar, J.B., Planer, S.L., Legasse, A., Sylwester, A.W., Piatak Jr., M., Lifson, J.D., Maino, V.C., Sodora, D.L., Douek, D.C., Axthelm, M.K., Grossman, Z., Picker, L.J., 2007. Progressive $CD4^+$ central memory T cell decline results in $CD4^+$ effector memory insufficiency and overt disease in chronic SIV infection. J. Exp. Med. 204, 2171–2185.

Okuma, K., Tanaka, R., Ogura, T., Ito, M., Kumakura, S., Yanaka, M., Nishizawa, M., Sugiura, W., Yamamoto, N., Tanaka, Y., 2008. Interleukin-4-transgenic hu-PBL-SCID mice: a model for the screening of antiviral drugs and immunotherapeutic agents against X4 HIV-1 viruses. J. Infect. Dis. 197, 134–141.

Pedroza-Martins, L., Gurney, K.B., Torbett, B.E., Uittenbogaart, C.H., 1998. Differential tropism and replication kinetics of human immunodeficiency virus type 1 isolates in thymocytes: coreceptor expression allows viral entry, but productive infection of distinct subsets is determined at the postentry level. J. Virol. 72, 9441–9452.

Roeth, J.F., Collins, K.L., 2006. Human immunodeficiency virus type 1 Nef: adapting to intracellular trafficking pathways. Microbiol. Mol. Biol. Rev. 70, 548–563.

Sallusto, F., Geginat, J., Lanzavecchia, A., 2004. Central memory and effector memory T cell subsets: function, generation, and maintenance. Annu. Rev. Immunol. 22, 745–763.

Sato, K., Aoki, J., Misawa, N., Daikoku, E., Sano, K., Tanaka, Y., Koyanagi, Y., 2008. Modulation of human immunodeficiency virus type 1 infectivity through incorporation of tetraspanin proteins. J. Virol. 82, 1021–1033.

Schnittman, S.M., Denning, S.M., Greenhouse, J.J., Justement, J.S., Baseler, M., Kurtzberg, J., Haynes, B.F., Fauci, A.S., 1990. Evidence for susceptibility of intrathymic T-cell precursors and their progeny carrying T-cell antigen receptor phenotypes $TCR\alpha\beta^+$ and $TCR\gamma\delta^+$ to human immunodeficiency virus infection: a mechanism for $CD4^+$ (T4) lymphocyte depletion. Proc. Natl. Acad. Sci. U. S. A. 87, 7727–7731.

Sereti, I., Sklar, P., Ramchandani, M.S., Read, S.W., Aggarwal, V., Imamichi, H., Natarajan, V., Metcalf, J.A., Kovacs, J.A., Tavel, J., Davey, R.T., Dersimonian, R., Lane, H.C., 2007. $CD4^+$ T cell responses to interleukin-2 administration in HIV-infected patients are

directly related to the baseline level of immune activation. J. Infect Dis. 196, 677–683.
Stevenson, M., Stanwick, T.L., Dempsey, M.P., Lamonica, C.A., 1990. HIV-1 replication is controlled at the level of T cell activation and proviral integration. EMBO J. 9, 1551–1560.
Traggiai, E., Chicha, L., Mazzucchelli, L., Bronz, L., Piffaretti, J.C., Lanzavecchia, A., Manz, M.G., 2004. Development of a human adaptive immune system in cord blood cell-transplanted mice. Science 304, 104–107.
Vatakis, D.N., Bristol, G., Wilkinson, T.A., Chow, S.A., Zack, J.A., 2007. Immediate activation fails to rescue efficient human immunodeficiency virus replication in quiescent $CD4^+$ T cells. J. Virol. 81, 3574–3582.
Wilpshaar, J., Falkenburg, J.H., Tong, X., Noort, W.A., Breese, R., Heilman, D., Kanhai, H., Orschell-Traycoff, C.M., Srour, E.F., 2000. Similar repopulating capacity of mitotically active and resting umbilical cord blood $CD34^+$ cells in NOD/SCID mice. Blood 96, 2100–2107.
Ye, P., Kirschner, D.E., Kourtis, A.P., 2004. The thymus during HIV disease: role in pathogenesis and in immune recovery. Curr. HIV Res. 2, 177–183.
Zack, J.A., Arrigo, S.J., Weitsman, S.R., Go, A.S., Haislip, A., Chen, I.S., 1990. HIV-1 entry into quiescent primary lymphocytes: molecular analysis reveals a labile, latent viral structure. Cell 61, 213–222.
Zhang, Z., Schuler, T., Zupancic, M., Wietgrefe, S., Staskus, K.A., Reimann, K.A., Reinhart, T.A., Rogan, M., Cavert, W., Miller, C.J., Veazey, R.S., Notermans, D., Little, S., Danner, S.A., Richman, D.D., Havlir, D., Wong, J., Jordan, H.L., Schacker, T.W., Racz, P., Tenner-Racz, K., Letvin, N.L., Wolinsky, S., Haase, A.T., 1999. Sexual transmission and propagation of SIV and HIV in resting and activated $CD4^+$ T cells. Science 286, 1353–1357.
Zhang, Z.Q., Wietgrefe, S.W., Li, Q., Shore, M.D., Duan, L., Reilly, C., Lifson, J.D., Haase, A.T., 2004. Roles of substrate availability and infection of resting and activated $CD4^+$ T cells in transmission and acute simian immunodeficiency virus infection. Proc. Natl. Acad. Sci. U. S. A. 101, 5640–5645.

Journal of General Virology (2010), 91, 773–781 DOI 10.1099/vir.0.017368-0

Small intestine CD4$^+$ cell reduction and enteropathy in simian/human immunodeficiency virus KS661-infected rhesus macaques in the presence of low viral load

Katsuhisa Inaba,[1] Yoshinori Fukazawa,[1] Kenta Matsuda,[1] Ai Himeno,[1] Megumi Matsuyama,[1] Kentaro Ibuki,[1] Yoshiharu Miura,[2] Yoshio Koyanagi,[2] Atsushi Nakajima,[3] Richard S. Blumberg,[4] Hidemi Takahashi,[5] Masanori Hayami,[1] Tatsuhiko Igarashi[1] and Tomoyuki Miura[1]

Correspondence
Tomoyuki Miura
tmiura@virus.kyoto-u.ac.jp

[1]Laboratory of Primate Model, Experimental Research Center for Infectious Diseases, Institute for Virus Research, Kyoto University, 53 Shogoinkawaramachi, Sakyo-ku, Kyoto 606-8507, Japan

[2]Laboratory of Viral Pathogenesis, Institute for Virus Research, Kyoto University, 53 Shogoinkawaramachi, Sakyo-ku, Kyoto 606-8507, Japan

[3]Division of Gastroenterology, Yokohama City University Graduate School of Medicine, Yokohama, Japan

[4]Division of Gastroenterology, Brigham and Women's Hospital, Harvard Medical School, Boston, MA, USA

[5]Department of Microbiology and Immunology, Nippon Medical School, Tokyo, Japan

Human immunodeficiency virus type 1, simian immunodeficiency virus and simian/human immunodeficiency virus (SHIV) infection generally lead to death of the host accompanied by high viraemia and profound CD4$^+$ T-cell depletion. SHIV clone KS661-infected rhesus macaques with a high viral load set point (HVL) ultimately experience diarrhoea and wasting at 6–12 months after infection. In contrast, infected macaques with a low viral load set point (LVL) usually live asymptomatically throughout the observation period, and are therefore referred to as asymptomatic LVL (Asym LVL) macaques. Interestingly, some LVL macaques exhibit diarrhoea and wasting similar to the symptoms of HVL macaques and are termed symptomatic LVL (Sym LVL) macaques. This study tested the hypothesis that Sym LVL macaques have the same degree of intestinal abnormalities as HVL macaques. The proviral DNA loads in lymphoid tissue and the intestines of Sym LVL and Asym LVL macaques were comparable and all infected monkeys showed villous atrophy. Notably, the CD4$^+$ cell frequencies of lymphoid tissues and intestines in Sym LVL macaques were remarkably lower than those in Asym LVL and uninfected macaques. Furthermore, Sym LVL and HVL macaques exhibited an increased number of activated macrophages. In conclusion, intestinal disorders including CD4$^+$ cell reduction and abnormal immune activation can be observed in SHIV-KS661-infected macaques independent of virus replication levels.

Received 5 October 2009
Accepted 3 November 2009

INTRODUCTION

The intestinal tract, which is the largest mucosal and lymphoid organ and which contains the majority of the total lymphocytes in the body, is an important port of entry for human immunodeficiency virus type 1 (HIV-1) infection in vertical and homosexual transmission (Smith *et al.*, 2003). Additionally, the intestinal tract is a central site in the interaction between HIV-1 and its host, and suffers profound pathological changes as a result of HIV-1 infection. HIV-1 infection of the intestinal tract is characterized by virus replication (Fackler *et al.*, 1998), CD4$^+$ T-cell depletion (Brenchley *et al.*, 2004), opportunistic infection and HIV enteropathy, which is an idiopathic intestinal disorder observed in infected patients with diarrhoea (Kotler, 2005). In particular, CD4$^+$ T-cell depletion, which is the immunological hallmark in the development of AIDS, preferentially takes place in the intestinal tract rather than in the peripheral blood throughout the infection (Brenchley *et al.*, 2004). This

observation is based on the following findings: (i) most naturally transmitted HIV-1 strains are chemokine receptor 5 (CCR5)-tropic; and (ii) the intestinal tract, especially the lamina propria, contains a large number of activated memory $CCR5^+$ $CD4^+$ T cells, which indicates a high susceptibility for HIV-1 infection, whereas the peripheral blood has a relatively small population of these cells (Anton *et al.*, 2000; Lapenta *et al.*, 1999). $CD4^+$ T-cell depletion from the intestinal tract by HIV-1 infection is thought to lead to progressive dysfunction of mucosal immunity, which triggers immunodeficiency (Paiardini *et al.*, 2008). In addition to $CD4^+$ T-cell depletion in the intestinal tract, HIV-1 infection causes histopathological changes in the intestine, including villous atrophy, crypt hyperplasia and acute/chronic inflammation (Batman *et al.*, 1989).

Chronic disease of the intestinal tract generally manifests as inflammation (Kahn, 1997). Diarrhoea is a major intestinal symptom caused by various stimuli to the intestinal tract such as pathogens, toxins and dysfunction of the immune system (Gibbons & Fuchs, 2007). Because HIV-1 infection weakens the host immune system, AIDS is one of the primary causes of chronic diarrhoea (Sestak, 2005). In developing countries, diarrhoea was a major symptom in advanced HIV-1 infection prior to the establishment of highly active antiretroviral therapy (HAART) (Wilcox & Saag, 2008). Dehydration and malabsorption as a result of chronic diarrhoea can lead to progressive weight loss and can contribute to morbidity and mortality in HIV-1-infected patients (Sharpstone & Gazzard, 1996). Therefore, chronic diarrhoea is one of the most important clinical signs in AIDS patients.

AIDS models using non-human primates have provided many important observations on AIDS pathogenesis. The first finding of early $CD4^+$ T-cell depletion from the intestinal tract was reported in a study using simian immunodeficiency virus (SIV)-infected macaques (Veazey *et al.*, 1998). Intestinal $CD4^+$ T cells of rhesus macaques predominantly exhibit a $CCR5^+$ activated memory phenotype, and $CD4^+$ T cells of this phenotype are selectively eliminated in SIV-infected macaques, indicating that the majority of intestinal $CD4^+$ T cells are primary targets of SIV infection (Veazey *et al.*, 2000a, b). Accordingly, detailed analysis of the intestinal tract using animal models is essential for an understanding of AIDS pathogenesis.

Simian/human immunodeficiency virus (SHIV)-KS661 is a molecular clone and a pathogenic virus in rhesus macaques. SHIV-KS661 systemically depletes $CD4^+$ T cells of rhesus macaques within 4 weeks of infection (Miyake *et al.*, 2006). Based on our observations over a number of years, intravenous infection of rhesus macaques with SHIV-KS661 consistently results in high viraemia and $CD4^+$ T-cell depletion, followed by malignant morbidity as a result of severe chronic diarrhoea and wasting after 6–18 months. Generally, the time to clinical morbidity in rhesus macaques infected with pathogenic SHIVs, such as SHIV-89.6P and SHIV-KS661, is considerably shorter than in HIV-1-infected humans, who take an average of 10 years to progress to AIDS. In addition, all subsets of $CD4^+$ T cells including memory and naïve T cells are thoroughly depleted in pathogenic SHIV-infected macaques. However, in the SHIV-KS661 macaque model, diarrhoea and wasting, which are major symptoms in advanced HIV-1 infection, can clearly be recognized and defined in association with disease progression.

Recently, we observed that, in many rhesus macaques infected intrarectally with SHIV-KS661, plasma viral RNA loads decreased gradually to undetectable levels in the chronic phase, which is quite different from the case with intravenous infection. It is well known that pathogenic SIV and SHIV infections in monkeys, like HIV-1 infections in humans, generally lead to high viraemia, profound $CD4^+$ T-cell depletion and death. Interestingly, in this study, two out of six intrarectally inoculated macaques with a low plasma viral load experienced malignant morbidity manifest as severe diarrhoea and wasting, similar to what we observed in infected macaques with high viraemia. The purpose of this study was to elucidate why macaques with a low plasma viral load experienced diarrhoea and wasting. As an explanation for this morbidity, we hypothesized that, even if the viral load set-point is suppressed, SHIV-KS661-infected macaques would have the same degree of intestinal abnormalities as infected macaques with high viraemia. To test this hypothesis, we analysed $CD4^+$ cell frequencies in lymphoid and intestinal tissues and damage to the intestinal mucosa in infected macaques with high and low viral load set points (HVL and LVL, respectively). Here, we have provided evidence for the development of intestinal disorders in SHIV-KS661-infected macaques irrespective of the plasma viral RNA load.

RESULTS

Diarrhoea and wasting in two macaques despite low viral load

All macaques inoculated intravenously with SHIV-KS661 and one out of seven macaques inoculated intrarectally with SHIV-KS661 exhibited high set points of plasma viral RNA loads, persisting at over 10^6 copies ml^{-1} until they needed to be euthanized as a result of diarrhoea and wasting (Fig. 1a). In contrast, in the remaining six macaques inoculated intrarectally with SHIV-KS661, the set points of plasma viral RNA load gradually decreased to undetectable levels (Fig. 1a). We called these macaques showing high and low set points of viral RNA load HVL and LVL macaques, respectively. During an observation period of approximately 1.4 years, two LVL macaques (MM397 and MM399) experienced severe diarrhoea and wasting and required euthanasia at approximately 22 weeks post-infection (p.i.), similar to HVL macaques, whereas the remaining four LVL macaques were asymptomatic (Fig. 1a). We termed the healthy LVL macaques asymptomatic LVL macaques (Asym LVL) and the LVL

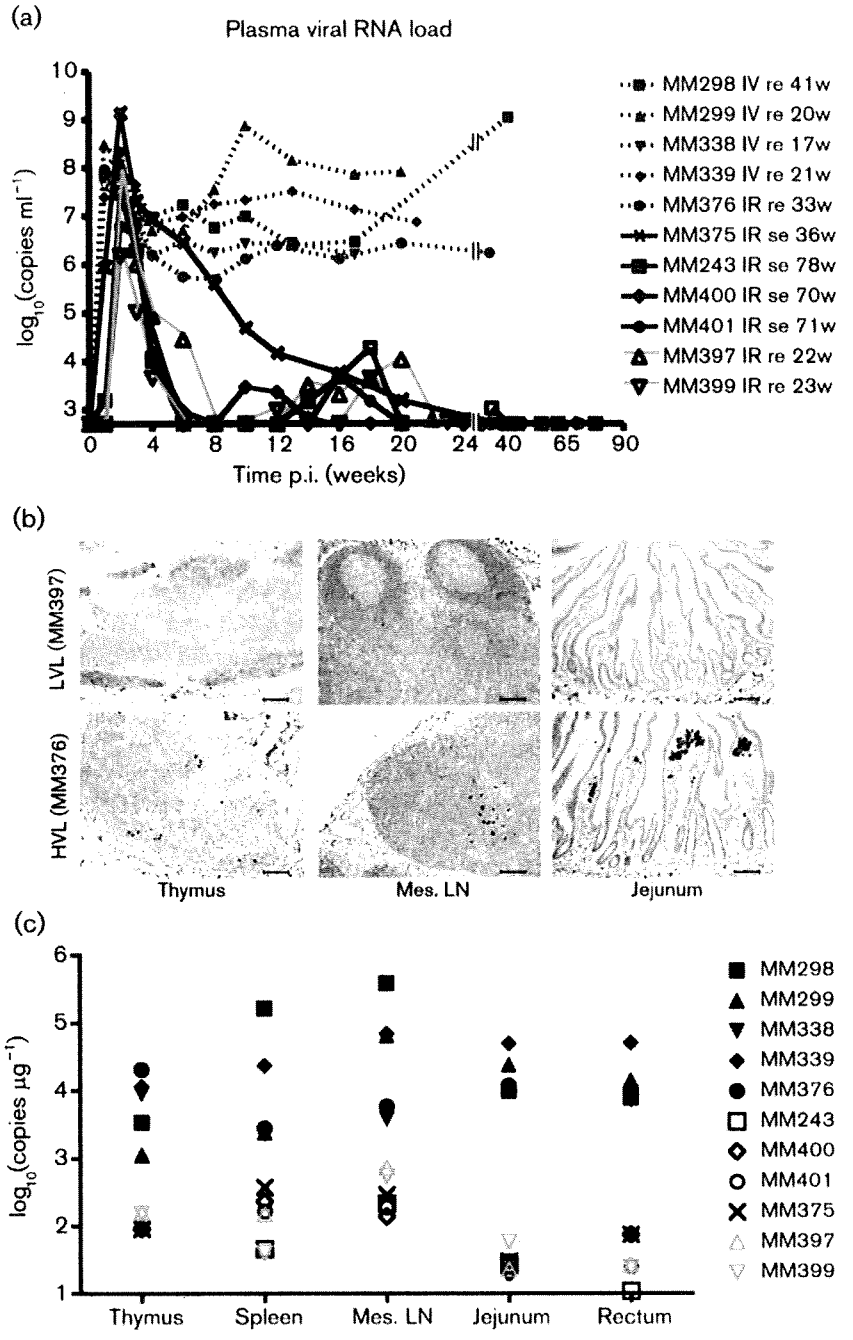

Fig. 1. Distribution of virus in various tissues of SHIV-KS661-infected rhesus macaques. (a) Time course of plasma viral RNA loads as measured by quantitative RT-PCR. The detection limit of plasma viral RNA loads was 500 copies ml^{-1}. The animal ID numbers, infection route and when and how they were euthanized are indicated on the figure. IV, Intravenous inoculation; IR, intrarectal inoculation; re, required euthanasia; se, scheduled euthanasia; w, number of weeks after infection when euthanasia was performed. (b) Immunohistochemical detection of Nef antigen in thymus, mesenteric lymph nodes (Mes. LN) and jejunum. Brown staining indicates Nef^+ cells. The upper panels show representative tissue sections from a Sym LVL macaque (MM397) and the lower panels show representative tissue sections from an HVL macaque (MM376). Bars, 100 µm. (c) Proviral DNA loads in different tissues of SHIV-KS661-infected macaques, as measured by quantitative PCR. The detection limit of proviral DNA loads was 10 copies μg^{-1}. Filled black symbols indicate HVL macaques, open black symbols indicate Asym LVL macaques and open grey symbols indicate Sym LVL macaques.

macaques with diarrhoea and wasting symptomatic LVL macaques (Sym LVL).

Antibody response against SHIV in infected macaques

The LVL macaques showed antibody responses to SHIV-KS661 at 3–4 weeks p.i. and then developed strong antibody responses that persisted up to 18 weeks p.i. (Table 1). In contrast, two of the HVL macaques (MM298 and MM299) showed no antibody response, whilst the remaining two (MM338 and MM339) showed very low antibody responses. Among the HVL macaques, only MM376 showed a strong antibody response: the titre reached 1:2048 at 6 weeks p.i., but then decreased to a much lower value. These results showed that LVL macaques succeeded in maintaining a strong antibody response, whilst HVL macaques failed to do so.

Viral levels in tissues from Sym LVL and Asym LVL macaques are not significantly different

To investigate whether the infected macaques had different viral levels in their lymphoid and intestinal tissues, we used

Table 1. Anti-HIV antibody titres in infected monkeys

– indicates a titre of <32.

Time (weeks)	Intrarectal inoculation						Intravenous inoculation			
	LVL						HVL			
	MM243	MM397	MM399	MM400	MM401	MM375	MM376	MM298	MM299	MM338	MM339
0	–	–	–	–	–	–	–	–	–	–	–
1	–	–	–	–	–	–	–	–	–	–	–
2	–	–	–	–	–	–	–	–	–	64	64
3	32	–	32	–	–	128	–	–	–	32	32
4	32	16384	32	64	32	512	512	–	–	–	–
6	8192	16384	256	64	4096	1024	2048	–	–	–	–
8	4096	16384	1024	128	1024	16384	512	–	–	–	–
10	16384	16384	2048	512	512	16384	512	–	–	–	–
12	16384	16384	256	512	4096	16384	512				
13								–	–	–	–
14	16384	16384	1024	512	2048						
16	4096	8192	1024	1024	1024	16384	64				
17								–	–	–	–
18	8192	16384	2048	8192	4096						

the Nef antigen as a marker of virus infection using immunohistochemistry and quantitative analysis of proviral DNA in lymphoid and intestinal tissues. Nef^+ cells were detected in large numbers in the tissues of HVL macaques, but were undetectable in both Sym LVL (Fig. 1b) and Asym LVL (data not shown) macaques.

In the HVL macaques, high proviral DNA loads (>1000 copies μg^{-1}) were found in all of the tissues examined (Fig. 1c). In contrast, the proviral DNA loads in the tissues of the LVL macaques were only several tens to several hundreds of copies μg^{-1} (Fig. 1c). Furthermore, Sym LVL and Asym LVL macaques exhibited comparably low proviral DNA loads in these tissues (Fig. 1c). The low viral levels in lymphoid and intestinal tissues in the LVL macaques were consistent with their set points of plasma viral RNA loads. The viral levels in lymphoid and intestinal tissues were not significantly different between Sym LVL and Asym LVL macaques.

Diarrhoea and wasting in LVL macaques correlate with $CD4^+$ cell frequency in lymphoid and intestinal tissues, but not in peripheral blood

Because $CD4^+$ T-cell depletion is the hallmark of AIDS, we first examined $CD4^+$ T-cell counts in peripheral blood. Whilst peripheral $CD4^+$ T cells were completely and irreversibly depleted in HVL macaques throughout the infection, they displayed various kinetics in LVL macaques (Fig. 2a). MM397 (Sym LVL) and MM401 (Asym LVL) had very low $CD4^+$ T-cell counts (<150 cells ml^{-1}) at all times at which they were examined after infection, whereas MM399 (Sym LVL) and MM400 (Asym LVL) maintained moderate $CD4^+$ T-cell counts (>300 cells ml^{-1}) throughout the experiment (Fig. 2a).

Naïve $CD4^+$ T cells of MM397 (Sym LVL), MM243 (Asm LVL) and MM401 (Asym LVL) were depleted as early as 4 weeks p.i., whereas those of MM399 (Sym LVL) and MM400 (Asym LVL) remained at moderate levels (Fig. 2b). The HVL macaques were not examined because their peripheral $CD4^+$ T cells were depleted.

In addition to evaluating $CD4^+$ T cells in the blood, we evaluated $CD4^+$ cells in lymphoid and intestinal tissues using CD4 staining. The HVL macaques showed severe depletion of $CD4^+$ cells in all lymphoid tissues and intestine compared with the uninfected macaques (Fig. 2c, d). Interestingly, the $CD4^+$ cell frequencies in the tissues were clearly lower in Sym LVL macaques than in uninfected macaques (Fig. 2c, d). However, the $CD4^+$ cell frequencies in the tissues of Asym LVL macaques were comparable to those in uninfected macaques. These findings indicated that the emergence of diarrhoea and wasting in LVL macaques correlated with the low $CD4^+$ cell frequency in lymphoid tissues and the intestines, but not with the counts of peripheral $CD4^+$ T-cell subsets.

Infected animals exhibit significantly shorter villi

Symptomatic animals (Sym LVL and HVL macaques) exhibited diarrhoea. To examine whether the jejunum of symptomatic animals exhibited the histopathological changes that suggest AIDS-related enteropathy, we measured villous length on haematoxylin and eosin (H&E)-stained samples of jejunum in uninfected and infected macaques. Surprisingly, villous length was significantly

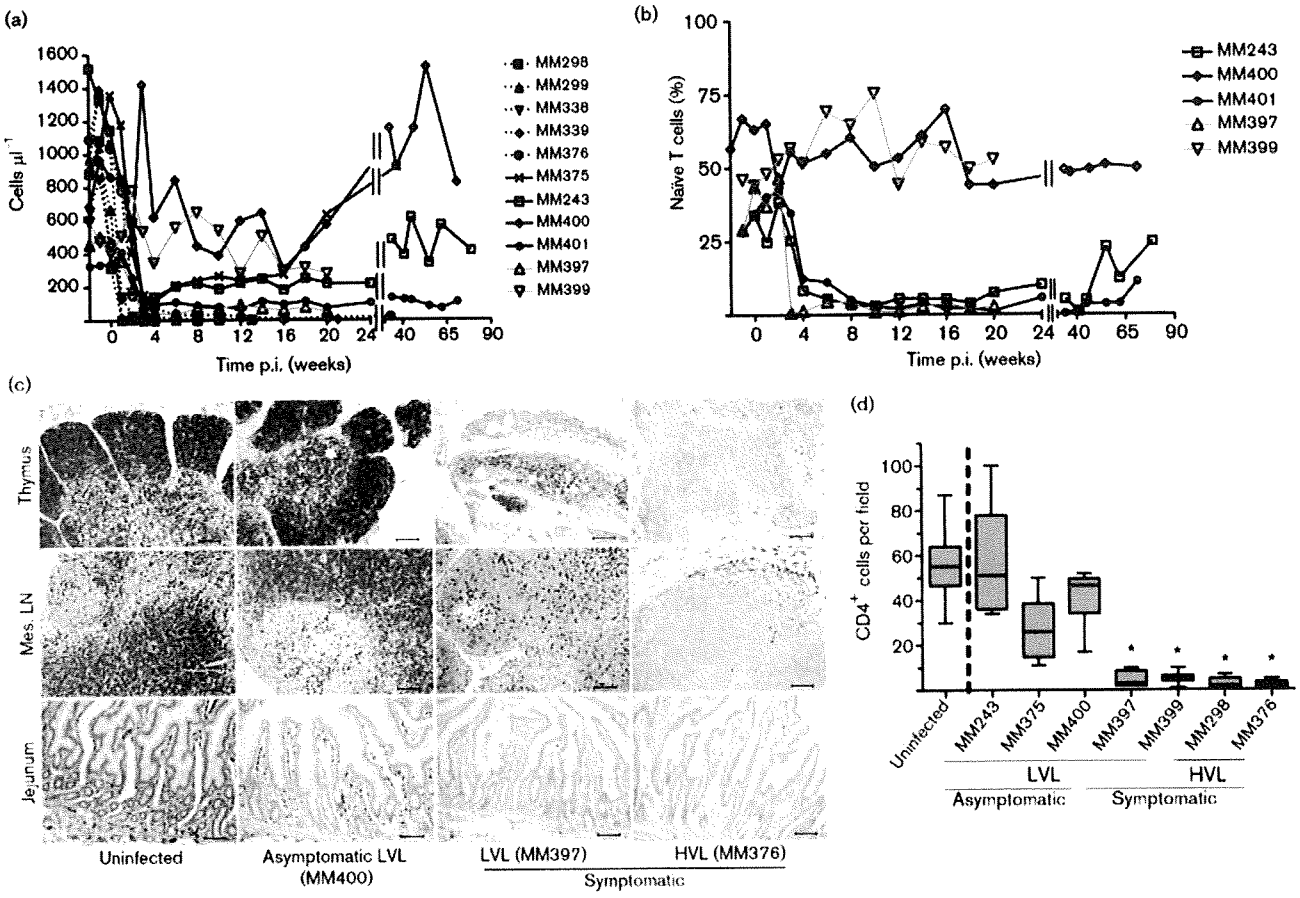

Fig. 2. Counts of circulating $CD4^+$ T-cell subsets and $CD4^+$ cell frequency in lymphoid and intestinal tissues at the time of euthanasia in SHIV-KS661-infected rhesus macaques. Counts of circulating $CD4^+$ T-cell subsets were analysed by flow cytometry and whole-blood counts. (a) Circulating $CD4^+$ T-cell counts. The ID numbers of the macaques are indicated on the figure. (b) Proportion of $CD95^+$ naïve cells in circulating $CD4^+$ T cells of LVL macaques. Solid black lines indicate Asym LVL macaques and solid grey lines indicate Sym LVL macaques. (c) $CD4^+$ cell frequencies in thymus, mesenteric lymph nodes (Mes. LN) and jejunum of representative uninfected, Asym LVL, Sym LVL and HVL macaques. Bars, 100 µm. (d) Quantification of jejunum $CD4^+$ cells in uninfected and infected macaques. The numbers of $CD4^+$ cells were enumerated in at least ten fields of the tissues at a magnification of 200×. Statistical analysis was performed using Student's *t*-test for the data from five uninfected and each infected macaque (*, $P<0.0001$). Data for MM299, MM338, MM339 and MM401 were not available.

shorter in all of the infected animals than in uninfected animals ($P<0.0001$) (Fig. 3a, b). This suggested that SHIV-infected animals develop villous atrophy, irrespective of viral load.

Increased number of activated macrophages in the jejunum of symptomatic animals

Macrophages appeared to be more abundant in H&E-stained jejunal sections in symptomatic animals. This was confirmed by CD68 staining: the frequency of $CD68^+$ macrophages in the jejunum was considerably higher in symptomatic animals than in uninfected animals, but was not significantly different between uninfected animals and Asym LVL macaques (data not shown). Furthermore, $CD68^+$ macrophages in the small intestine of Sym LVL and HVL macaques appeared to be activated because their size was increased. To examine whether the number of activated $CD68^+$ macrophages increased in the small intestine, we double stained for CD68 and Ki67 in the small intestine sections by immunohistochemistry. The frequency of $CD68^+$ $Ki67^+$ macrophages in the jejunum of all symptomatic animals examined was significantly higher than that of uninfected animals ($P<0.0001$) (Fig. 3c, d). This suggested that abnormal activation of intestinal macrophages occurred in symptomatic animals irrespective of viral load.

DISCUSSION

It is important to discuss initially why some SHIV-infected macaques had an HVL at the late stage, whilst others had

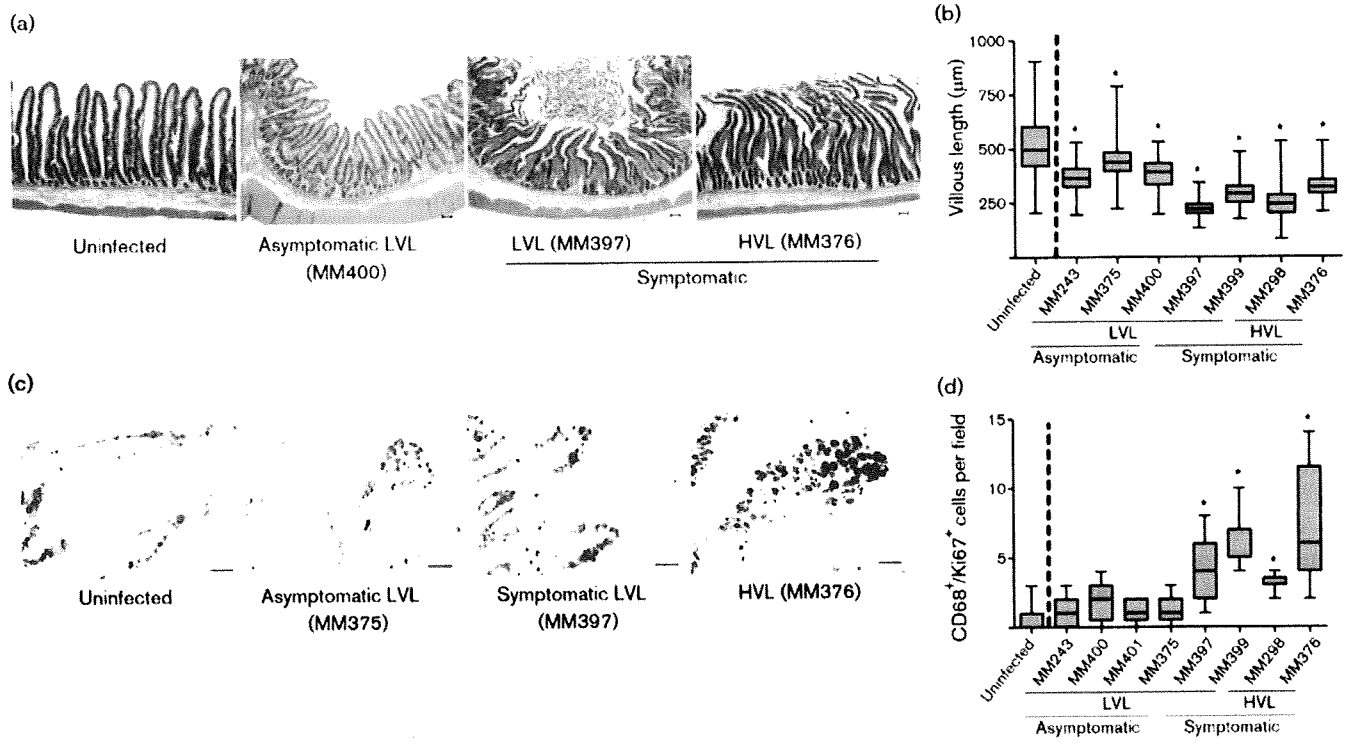

Fig. 3. Villous length in jejunum and counts of activated macrophages in the small intestine at the time of euthanasia in SHIV-KS661-infected rhesus macaques. (a) H&E-stained sections of jejunum of representative uninfected, Asym LVL, Sym LVL and HVL macaques. Bars, 200 μm. (b) Comparison of villous length in uninfected and infected macaques. The lengths of at least 100 villi were measured in each macaque. Statistical analysis was performed using Student's *t*-test for the data from four uninfected and each infected macaque (*, $P<0.0001$). Data for MM299, MM338, MM339 and MM401 were not available. (c) Ki67 and CD68 staining in the small intestine of representative uninfected, Asym LVL, Sym LVL and HVL macaques. Brown staining indicates $Ki67^+$ cells and blue staining indicates $CD68^+$ cells. Bar, 50 μm. (d) Comparison of $CD68^+$ $Ki67^+$ cell counts in uninfected and infected macaques. The numbers of $CD68^+$ $Ki67^+$ cells were enumerated in at least ten fields of the tissues at a magnification of 200×. Statistical analysis was performed using Student's *t*-test for the data from seven uninfected and each infected macaque (*, $P<0.0001$). Data for MM299, MM338 and MM339 were not available.

an LVL. The LVL macaques had much stronger antibody responses than the HVL macaques (Table 1). SHIV-89.6P is easily controlled by the antibody response (Montefiori *et al.*, 1998). SHIV-KS661, which shares its genetic origin with SHIV-89.6P, might be strongly affected by the antibody response. Virus replication during the primary phase clearly occurred later in the intrarectally inoculated macaques than in the intravenously inoculated macaques. Therefore, this delay might contribute to the continuous and strong antibody response in the intrarectally inoculated macaques, consequently resulting in a low viral load in most of the intrarectally inoculated macaques.

The purpose of this study was to elucidate why LVL macaques experience diarrhoea and wasting. A comparison of circulating $CD4^+$ T-cell counts (Fig. 2a) and relative levels of naïve T-cells (Fig. 2b) in LVL macaques did not reveal a substantial difference between Sym LVL (which showed diarrhoea and wasting) and Asym LVL (which were healthy) macaques. The villous length in the intestine also did not affect the level of malignancy of the disease condition, as all infected monkeys showed significant villous atrophy, suggesting a high sensitivity to infection itself. However, Sym LVL and HVL macaques exhibited two findings that Asym LVL macaques did not: (i) $CD4^+$ cell reduction in intestinal and lymphoid tissues (Fig. 2c, d), a hallmark of AIDS; and (ii) abnormal innate immune activation, which was reflected by an increased number of activated macrophages within the intestines (Fig. 3c, d). Ki67 serves as a proliferation marker and proliferation of macrophages may seem unlikely. However, there are some reports about local macrophage proliferation in inflammation sites, indicating the infiltration of activated macrophages associated with tissue damage (Isbel *et al.*, 2001; Norton, 1999). These observations indicated the existence of immunopathological disorders in the intestines not only in HVL macaques but also in Sym LVL macaques.

Many studies have shown positive correlations between the development of AIDS and some characteristic features in

the intestinal tracts of HIV-1-infected humans and pathogenic SIV- or SHIV-infected monkeys: continuous $CD4^+$ T-cell depletion (Brenchley *et al.*, 2004; Ling *et al.*, 2007), abnormal and chronic immune activation (Brenchley *et al.*, 2006; Hazenberg *et al.*, 2003) and enteropathy (Kotler, 2005). Immune activation (as shown by an increased number of intestinal activated macrophages) and intestinal $CD4^+$ cell depletion in Sym LVL macaques strongly suggest the presence of an AIDS-like disease in this subset of animals. Hence, these results suggest that an AIDS-like intestinal disease can occur in LVL macaques despite their low viral load, as well as in HVL macaques.

Some HIV-1-infected patients experience poor recovery of circulating $CD4^+$ T cells, even when their plasma HIV-1 RNA load is suppressed by HAART (Kaufmann *et al.*, 2003; Marchetti *et al.*, 2006; Piketty *et al.*, 1998). These individuals are called immunological non-responders (Marchetti *et al.*, 2006), and have been found to have increased plasma lipopolysaccharide levels, suggesting that bacteria had been translocated from the intestines into the circulation with concomitant activation of T-cell compartments (Marchetti *et al.*, 2006, 2008). Furthermore, some patients who maintain an undetectable or nearly undetectable plasma viral RNA load in the absence of HAART also develop AIDS disease progression (Madec *et al.*, 2005) and have abnormal immune activation and increased plasma lipopolysaccharide levels (Hunt *et al.*, 2008). These observations may indicate that disease progression in a subset of HIV-1-infected individuals is independent of viraemia. Accordingly, the disease progression under conditions of low viral load that we observed in SHIV-KS661-infected macaques can also occur in HIV-1-infected individuals.

Consistent with the fact that intestinal $CD4^+$ cell depletion triggers mucosal immune dysfunction, a notable difference observed between Sym LVL and Asym LVL macaques was the low $CD4^+$ cell frequency in the intestines of the Sym LVL macaques. We propose that the intestinal $CD4^+$ cells in Sym LVL macaques were not able to recover after intestinal $CD4^+$ cell reduction during the early phases of infection. We reported previously that SHIV-KS661 infection of rhesus macaques caused early intestinal $CD4^+$ T-cell depletion (Fukazawa *et al.*, 2008; Miyake *et al.*, 2006). Although we did not examine the macaques during the early phases of infection, the intestinal $CD4^+$ T cells of both Sym LVL and Asym LVL macaques should have been depleted at this time, as even moderately pathogenic SHIV can cause intestinal $CD4^+$ cell reduction during the early phase of infection (Fukazawa *et al.*, 2008). Therefore, the near-normal frequency of intestinal $CD4^+$ cells in Asym LVL macaques would be the result of $CD4^+$ cell recovery after intestinal $CD4^+$ cell reduction during the early phase of infection. In contrast, intestinal $CD4^+$ cells in Sym LVL macaques may be unable to recover, even though virus replication has been controlled. Similarly, intestinal $CD4^+$ cell recovery was found to be important for halting disease progression in SIVmac239-infected rhesus macaques (Ling *et al.*, 2007). Accordingly, one of the important determinants for disease progression in SHIV-KS661-infected macaques may be $CD4^+$ cell recovery in the intestines.

We further hypothesize that this inappropriately low level of $CD4^+$ cells within the intestines of the SHIV-KS661-infected animals (and phenotypically similar humans) is permissive to the excessive activation of resident tissue macrophages. One implication of these studies is that regulatory T-cell subsets of $CD4^+$ cells may be especially vulnerable to this depletion, thus allowing this macrophage activation in view of the well-known role of regulatory T cells in inhibiting innate immune responses (Maloy *et al.*, 2003). This hypothesis will be important to assess in future studies to understand the pathophysiology in the intestines during the chronic phase of HIV-1 infection.

Taken together, the present results suggest that $CD4^+$ cell reduction and enteropathy can occur in SHIV-KS661-infected rhesus macaques even when the viral load is low. The ability or inability to restore intestinal $CD4^+$ cells may be a key factor determining disease progression, irrespective of virus replication levels in the chronic phase of SHIV-KS661 infection. The reason that the recovery of intestinal $CD4^+$ cells is impeded is unknown, although we can speculate on some possibilities such as the co-existence of other infectious microbial agents or impaired T-cell reconstitution caused by damage during thymopoiesis at an early phase of SHIV infection (Motohara *et al.*, 2006). We demonstrated comparable proviral DNA loads in the examined tissues between Sym and Asym LVL macaques, although the $CD4^+$ cell frequencies in the tissues were clearly reduced in Sym LVL macaques. Therefore, the quantity of provirus per CD4 cell in the tissues of Sym LVL macaques is considered to be relatively higher than that of Asym LVL macaques, and low-level replication that may be undetectable in the plasma viral load might be maintained in Sym LVL but not in Asym LVL macaques. Identifying the mechanisms of poor recovery of intestinal $CD4^+$ cells is needed to understand AIDS pathogenesis, because, as stated above, some HIV-1-infected patients have low $CD4^+$ T-cell counts even when viraemia is controlled. One useful approach is comparative and periodical analysis, including cellular immunology data, of the intestinal tract of the same animals from the early to the chronic phases using Sym LVL and Asym LVL macaques in this SHIV infection macaque model.

METHODS

Virus, animals and sample collection. Highly pathogenic SHIV-KS661 is a molecular clone of SHIV-C2/1 (GenBank accession no. AF217181), which was derived through *in vivo* passages of SHIV-89.6 (Shinohara *et al.*, 1999). The virus stock was prepared from the supernatant of virus-infected CEMx174 and M8166 human lymphoid cell lines.

All rhesus macaques used in this study were treated in accordance with the institutional regulations approved by the Committee for

Experimental Use of Non-human Primates in the Institute for Virus Research, Kyoto University, Japan. All macaques were inoculated with 2×10^3 50 % tissue culture infectious dose of SHIV-KS661 measured with CEMx174. The animal ID numbers, infection route and when they were euthanized are provided in Fig. 1(a).

Blood was collected periodically using sodium citrate as an anti-coagulant and examined by flow cytometry and for quantification of plasma viral RNA load. Tissue samples were obtained at the time of euthanasia and were used for quantification of proviral DNA and histopathology.

Determination of plasma viral RNA and proviral DNA loads. The viral loads in plasma and proviral DNA loads in lymphoid and intestinal tissues were determined by quantitative RT-PCR and quantitative PCR, respectively, as described previously (Motohara *et al.*, 2006). DNA samples were extracted directly from frozen tissue sections of each monkey using a DNeasy Tissue kit (Qiagen) according to the manufacturer's protocol.

Determination of antibody titres. Anti-HIV antibody titres were determined using a commercial particle agglutination kit (Serodia-HIV1/2; Fujirebio). Isolated plasma samples were serially diluted and assayed. The end point of the highest dilution giving a positive result was determined as the titre.

Flow cytometry. Flow cytometry was performed as described previously (Motohara *et al.*, 2006). Briefly, $CD4^+$ T cells were analysed by a combination of fluorescein isothiocyanate (FITC)-conjugated anti-monkey CD3 (clone FN-18; BioSource) and phycoerythrin-conjugated anti-human CD4 (clone NU-TH/I; Nichirei), and subsets of naïve and memory $CD4^+$ cells were analysed by a combination of FITC-conjugated anti-human CD95 (clone DX2; BD Pharmingen) and allophycocyanin-conjugated anti-human CD4 (clone L200; BD Pharmingen). $CD95^-$ $CD4^+$ cells were defined as naïve $CD4^+$ T cells and $CD95^+$ $CD4^+$ cells were defined as memory $CD4^+$ T cells. Labelled lymphocytes were examined on a FACSCalibur analyser using CellQuest software (BD Biosciences).

Histology and immunohistochemistry. Tissue samples were fixed in 4 % paraformaldehyde in PBS at 4 °C overnight and embedded in paraffin wax. Sections (4 μm) were dewaxed using xylene, rehydrated through an alcohol gradient, and stained with H&E. The villous length of the jejunum was measured with a micrometer. At least 40 villi from each section were measured.

For immunohistochemistry, sections were rehydrated and processed for 10 min in an autoclave in 10 mM citrate buffer (pH 6.0) to unmask the antigens, sequentially treated with TBS/Tween 20 (TBST) and aqueous hydrogen peroxide, left at 4 °C overnight or at room temperature for 30 min or 1 h for primary antibody reactions, washed with TBST, incubated at room temperature for 1 h with an Envision+ kit (a horseradish peroxidase-labelled anti-mouse immunoglobulin polymer; Dako), visualized using diaminobenzidine (DAB) substrate (Dako) as a chromogen, rinsed in distilled water, counterstained with haematoxylin and analysed by light microscopy (Biozero BZ-8000: Keyence).

For double staining (CD68 and Ki67) of sections, appropriately processed sections were incubated at room temperature for 1 h with unlabelled anti-Ki67 antibody at a dilution of 1:2000, the highly sensitive tyramide amplification step (CSAII; Dako) was performed, the slides were reacted with DAB to visualize the results and incubated with unlabelled anti-CD68 antibody at 4 °C overnight followed by incubation at room temperature for 1 h with Histofine Simple Stain AP (an alkaline phosphatase-labelled anti-mouse immunoglobulin polymer (Nichirei), and the results were visualized with a Blue Alkaline Phosphatase Substrate kit III (Vector Laboratories). Measurements of $CD68^+$ $Ki67^+$ cell counts were performed in ten fields at a magnification of 200 × by light microscopy.

Primary antibodies used in immunohistochemistry were anti-human CD4 (diluted 1:30; clone NCL-CD4; Novacastra Laboratories), anti-SIV Nef (diluted 1:500; FIT Biotech), anti-human CD68 (diluted 1:50; clone KP-1; Dako) and anti-human Ki67 (Ki-S5; Dako).

Statistical analysis. The significance of $CD4^+$ or $CD68^+$ $Ki67^+$ cell frequency measurements and villous length in the jejunum of infected monkeys compared with uninfected monkeys was analysed using an unpaired Student's *t*-test (two-tailed) using GraphPad Prism 4.0E software (Varsity Wave).

ACKNOWLEDGEMENTS

We are grateful to Dr James Raymond for editing the English of this manuscript; to Takahito Kazama, Reii Horiuchi, Noriko Nakajima and Tetsutaro Sata for technical support; to Dr Michael A. Eckhaus for histopathological interpretation; and to Takeshi Kobayashi for critical reading. This work was supported, in part, by Research on HIV/AIDS in Health and Labour Sciences Research Grants from the Ministry of Health, Labour and Welfare, Japan; a Grant-in-Aid for Scientific Research from the Ministry of Education and Science, Japan; a Research Grant for AIDS on Health Sciences focusing on Drug Innovation from the Japan Health Sciences Foundation; and a Program for the Promotion of Fundamental Studies in Health Sciences of the National Institute of Biomedical Innovation (NIBIO) of Japan.

REFERENCES

Anton, P. A., Elliott, J., Poles, M. A., McGowan, I. M., Matud, J., Hultin, L. E., Grovit-Ferbas, K., Mackay, C. R., Chen, I. S. Y. & Giorgi, J. V. (2000). Enhanced levels of functional HIV-1 co-receptors on human mucosal T cells demonstrated using intestinal biopsy tissue. *AIDS* **14**, 1761–1765.

Batman, P. A., Miller, A. R., Forster, S. M., Harris, J. R., Pinching, A. J. & Griffin, G. E. (1989). Jejunal enteropathy associated with human immunodeficiency virus infection: quantitative histology. *J Clin Pathol* **42**, 275–281.

Brenchley, J. M., Schacker, T. W., Ruff, L. E., Price, D. A., Taylor, J. H., Beilman, G. J., Nguyen, P. L., Khoruts, A., Larson, M. & other authors (2004). $CD4^+$ T cell depletion during all stages of HIV disease occurs predominantly in the gastrointestinal tract. *J Exp Med* **200**, 749–759.

Brenchley, J. M., Price, D. A., Schacker, T. W., Asher, T. E., Silvestri, G., Rao, S., Kazzaz, Z., Bornstein, E., Lambotte, O. & other authors (2006). Microbial translocation is a cause of systemic immune activation in chronic HIV infection. *Nat Med* **12**, 1365–1371.

Fackler, O. T., Schafer, M., Schmidt, W., Zippel, T., Heise, W., Schneider, T., Zeitz, M., Riecken, E. O., Mueller-Lantzsch, N. & Ullrich, R. (1998). HIV-1 p24 but not proviral load is increased in the intestinal mucosa compared with the peripheral blood in HIV-infected patients. *AIDS* **12**, 139–146.

Fukazawa, Y., Miyake, A., Ibuki, K., Inaba, K., Saito, N., Motohara, M., Horiuchi, R., Himeno, A., Matsuda, K. & other authors (2008). Small intestine $CD4^+$ T cells are profoundly depleted during acute simian–human immunodeficiency virus infection, regardless of viral pathogenicity. *J Virol* **82**, 6039–6044.

Gibbons, T. & Fuchs, G. J. (2007). Chronic enteropathy: clinical aspects. *Nestle Nutr Workshop Ser Pediatr Program* **59**, 89–101.

Hazenberg, M. D., Otto, S. A., van Benthem, B. H., Roos, M. T., Coutinho, R. A., Lange, J. M., Hamann, D., Prins, M. & Miedema, F.

(2003). Persistent immune activation in HIV-1 infection is associated with progression to AIDS. *AIDS* **17**, 1881–1888.

Hunt, P. W., Brenchley, J., Sinclair, E., McCune, J. M., Roland, M., Page-Shafer, K., Hsue, P., Emu, B., Krone, M. & other authors (2008). Relationship between T cell activation and $CD4^+$ T cell count in HIV-seropositive individuals with undetectable plasma HIV RNA levels in the absence of therapy. *J Infect Dis* **197**, 126–133.

Isbel, N. M., Nikolic-Paterson, D. J., Hill, P. A., Dowling, J. & Atkins, R. C. (2001). Local macrophage proliferation correlates with increased renal M-CSF expression in human glomerulonephritis. *Nephrol Dial Transplant* **16**, 1638–1647.

Kahn, E. (1997). Gastrointestinal manifestations in pediatric AIDS. *Pediatr Pathol Lab Med* **17**, 171–208.

Kaufmann, G. R., Perrin, L., Pantaleo, G., Opravil, M., Furrer, H., Telenti, A., Hirschel, B., Ledergerber, B., Vernazza, P. & other authors (2003). CD4 T-lymphocyte recovery in individuals with advanced HIV-1 infection receiving potent antiretroviral therapy for 4 years: the Swiss HIV Cohort Study. *Arch Intern Med* **163**, 2187–2195.

Kotler, D. P. (2005). HIV infection and the gastrointestinal tract. *AIDS* **19**, 107–117.

Lapenta, C., Boirivant, M., Marini, M., Santini, S. M., Logozzi, M., Viora, M., Belardelli, F. & Fais, S. (1999). Human intestinal lamina propria lymphocytes are naturally permissive to HIV-1 infection. *Eur J Immunol* **29**, 1202–1208.

Ling, B., Veazey, R. S., Hart, M., Lackner, A. A., Kuroda, M., Pahar, B. & Marx, P. A. (2007). Early restoration of mucosal CD4 memory CCR5 T cells in the gut of SIV-infected rhesus predicts long term non-progression. *AIDS* **21**, 2377–2385.

Madec, Y., Boufassa, F., Porter, K. & Meyer, L. (2005). Spontaneous control of viral load and CD4 cell count progression among HIV-1 seroconverters. *AIDS* **19**, 2001–2007.

Maloy, K. J., Salaun, L., Cahill, R., Dougan, G., Saunders, N. J. & Powrie, F. (2003). $CD4^+CD25^+$ T_R cells suppress innate immune pathology through cytokine-dependent mechanisms. *J Exp Med* **197**, 111–119.

Marchetti, G., Gori, A., Casabianca, A., Magnani, M., Franzetti, F., Clerici, M., Perno, C. F., Monforte, A., Galli, M. & Meroni, L. (2006). Comparative analysis of T-cell turnover and homeostatic parameters in HIV-infected patients with discordant immune-virological responses to HAART. *AIDS* **20**, 1727–1736.

Marchetti, G., Bellistri, G. M., Borghi, E., Tincati, C., Ferramosca, S., La Francesca, M., Morace, G., Gori, A. & Monforte, A. D. (2008). Microbial translocation is associated with sustained failure in $CD4^+$ T-cell reconstitution in HIV-infected patients on long-term highly active antiretroviral therapy. *AIDS* **22**, 2035–2038.

Miyake, A., Ibuki, K., Enose, Y., Suzuki, H., Horiuchi, R., Motohara, M., Saito, N., Nakasone, T., Honda, M. & other authors (2006). Rapid dissemination of a pathogenic simian/human immunodeficiency virus to systemic organs and active replication in lymphoid tissues following intrarectal infection. *J Gen Virol* **87**, 1311–1320.

Montefiori, D. C., Reimann, K. A., Wyand, M. S., Manson, K., Lewis, M. G., Collman, R. G., Sodroski, J. G., Bolognesi, D. P. & Letvin, N. L. (1998). Neutralizing antibodies in sera from macaques infected with chimeric simian–human immunodeficiency virus containing the envelope glycoproteins of either a laboratory-adapted variant or a primary isolate of human immunodeficiency virus type 1. *J Virol* **72**, 3427–3431.

Motohara, M., Ibuki, K., Miyake, A., Fukazawa, Y., Inaba, K., Suzuki, H., Masuda, K., Minato, N., Kawamoto, H. & other authors (2006). Impaired T-cell differentiation in the thymus at the early stages of acute pathogenic chimeric simian–human immunodeficiency virus (SHIV) infection in contrast to less pathogenic SHIV infection. *Microbes Infect* **8**, 1539–1549.

Norton, W. T. (1999). Cell reactions following acute brain injury: a review. *Neurochem Res* **24**, 213–218.

Paiardini, M., Frank, I., Pandrea, I., Apetrei, C. & Silvestri, G. (2008). Mucosal immune dysfunction in AIDS pathogenesis. *AIDS Rev* **10**, 36–46.

Piketty, C., Castiel, P., Belec, L., Batisse, D., Si Mohamed, A., Gilquin, J., Gonzalez-Canali, G., Jayle, D., Karmochkine, M. & other authors (1998). Discrepant responses to triple combination antiretroviral therapy in advanced HIV disease. *AIDS* **12**, 745–750.

Sestak, K. (2005). Chronic diarrhea and AIDS: insights into studies with non-human primates. *Curr HIV Res* **3**, 199–205.

Sharpstone, D. & Gazzard, B. (1996). Gastrointestinal manifestations of HIV infection. *Lancet* **348**, 379–383.

Shinohara, K., Sakai, K., Ando, S., Ami, Y., Yoshino, N., Takahashi, E., Someya, K., Suzaki, Y., Nakasone, T. & other authors (1999). A highly pathogenic simian/human immunodeficiency virus with genetic changes in cynomolgus monkey. *J Gen Virol* **80**, 1231–1240.

Smith, P. D., Meng, G., Salazar-Gonzalez, J. F. & Shaw, G. M. (2003). Macrophage HIV-1 infection and the gastrointestinal tract reservoir. *J Leukoc Biol* **74**, 642–649.

Veazey, R. S., DeMaria, M., Chalifoux, L. V., Shvetz, D. E., Pauley, D. R., Knight, H. L., Rosenzweig, M., Johnson, R. P., Desrosiers, R. C. & Lackner, A. A. (1998). Gastrointestinal tract as a major site of $CD4^+$ T cell depletion and viral replication in SIV infection. *Science* **280**, 427–431.

Veazey, R. S., Mansfield, K. G., Tham, I. C., Carville, A. C., Shvetz, D. E., Forand, A. E. & Lackner, A. A. (2000a). Dynamics of CCR5 expression by $CD4^+$ T cells in lymphoid tissues during simian immunodeficiency virus infection. *J Virol* **74**, 11001–11007.

Veazey, R. S., Tham, I. C., Mansfield, K. G., DeMaria, M., Forand, A. E., Shvetz, D. E., Chalifoux, L. V., Sehgal, P. K. & Lackner, A. A. (2000b). Identifying the target cell in primary simian immunodeficiency virus (SIV) infection: highly activated memory $CD4^+$ T cells are rapidly eliminated in early SIV infection in vivo. *J Virol* **74**, 57–64.

Wilcox, C. M. & Saag, M. S. (2008). Gastrointestinal complications of HIV infection: changing priorities in the HAART era. *Gut* **57**, 861–870.

Retrovirology

BioMed Central

Short report

Comparative study on the effect of human BST-2/Tetherin on HIV-1 release in cells of various species

Kei Sato[1], Seiji P Yamamoto[1,2], Naoko Misawa[1], Takeshi Yoshida[1], Takayuki Miyazawa[3] and Yoshio Koyanagi*[1]

Address: [1]Laboratory of Viral Pathogenesis, Institute for Virus Research, Kyoto University, Kyoto, Kyoto 606-8507, Japan, [2]Department of Molecular and Cellular Biology, Graduate School of Biostudies, Kyoto University, Kyoto, Kyoto 606-8501, Japan and [3]Laboratory of Viral Pathogenesis, Center for Emerging Virus Research, Institute for Virus Research, Kyoto University, Kyoto, Kyoto 606-8507, Japan

Email: Kei Sato - ksato@virus.kyoto-u.ac.jp; Seiji P Yamamoto - syamamot@virus.kyoto-u.ac.jp; Naoko Misawa - nmisawa@virus.kyoto-u.ac.jp; Takeshi Yoshida - tkyoshid@virus.kyoto-u.ac.jp; Takayuki Miyazawa - tmiyazaw@virus.kyoto-u.ac.jp; Yoshio Koyanagi* - ykoyanag@virus.kyoto-u.ac.jp

* Corresponding author

Published: 2 June 2009

Retrovirology 2009, **6**:53 doi:10.1186/1742-4690-6-53

Received: 3 February 2009
Accepted: 2 June 2009

This article is available from: http://www.retrovirology.com/content/6/1/53

Abstract

In this study, we first demonstrate that endogenous hBST-2 is predominantly expressed on the plasma membrane of a human T cell line, MT-4 cells, and that Vpu-deficient HIV-1 was less efficiently released than wild-type HIV-1 from MT-4 cells. In addition, surface hBST-2 was rapidly down-regulated in wild-type but not Vpu-deficient HIV-1-infected cells. This is a direct insight showing that provirus-encoded Vpu has the potential to down-regulate endogenous hBST-2 from the surface of HIV-1-infected T cells. Corresponding to previous reports, the aforementioned findings suggested that hBST-2 has the potential to suppress the release of Vpu-deficient HIV-1. However, the molecular mechanism(s) for tethering HIV-1 particles by hBST-2 remains unclear, and we speculated about the requirement for cellular co-factor(s) to trigger or assist its tethering ability. To explore this possibility, we utilize several cell lines derived from various species including human, AGM, dog, cat, rabbit, pig, mink, potoroo, and quail. We found that ectopic hBST-2 was efficiently expressed on the surface of all analyzed cells, and its expression suppressed the release of viral particles in a dose-dependent manner. These findings suggest that hBST-2 can tether HIV-1 particles without the need of additional co-factor(s) that may be expressed exclusively in primates, and thus, hBST-2 can also exert its function in many cells derived from a broad range of species. Interestingly, the suppressive effect of hBST-2 on HIV-1 release in Vero cells was much less pronounced than in the other examined cells despite the augmented surface expression of ectopic hBST-2 on Vero cells. Taken together, our findings suggest the existence of certain cell types in which hBST-2 cannot efficiently exert its inhibitory effect on virus release. The cell type-specific effect of hBST-2 may be critical to elucidate the mechanism of BST-2-dependent suppression of virus release.

Findings

To accomplish efficient release of HIV-1 particles, HIV-1 Vpu is required in certain cells (e.g., HeLa cells) but is dispensable in other cell types (e.g., HEK293 and Cos-7 cells) [1-3]. A previous report suggested that an inhibitory factor(s) for HIV-1 release is expressed in HeLa cells and the